Electronic Supplementary Material (ESI) for ChemComm.

Supporting Information

Water-soluble small-molecular probes for RNA based on two-photon fluorescence "off-on" process: Systematic analysis on live cell imaging and understanding on structure-activity relationships

Experimental Section

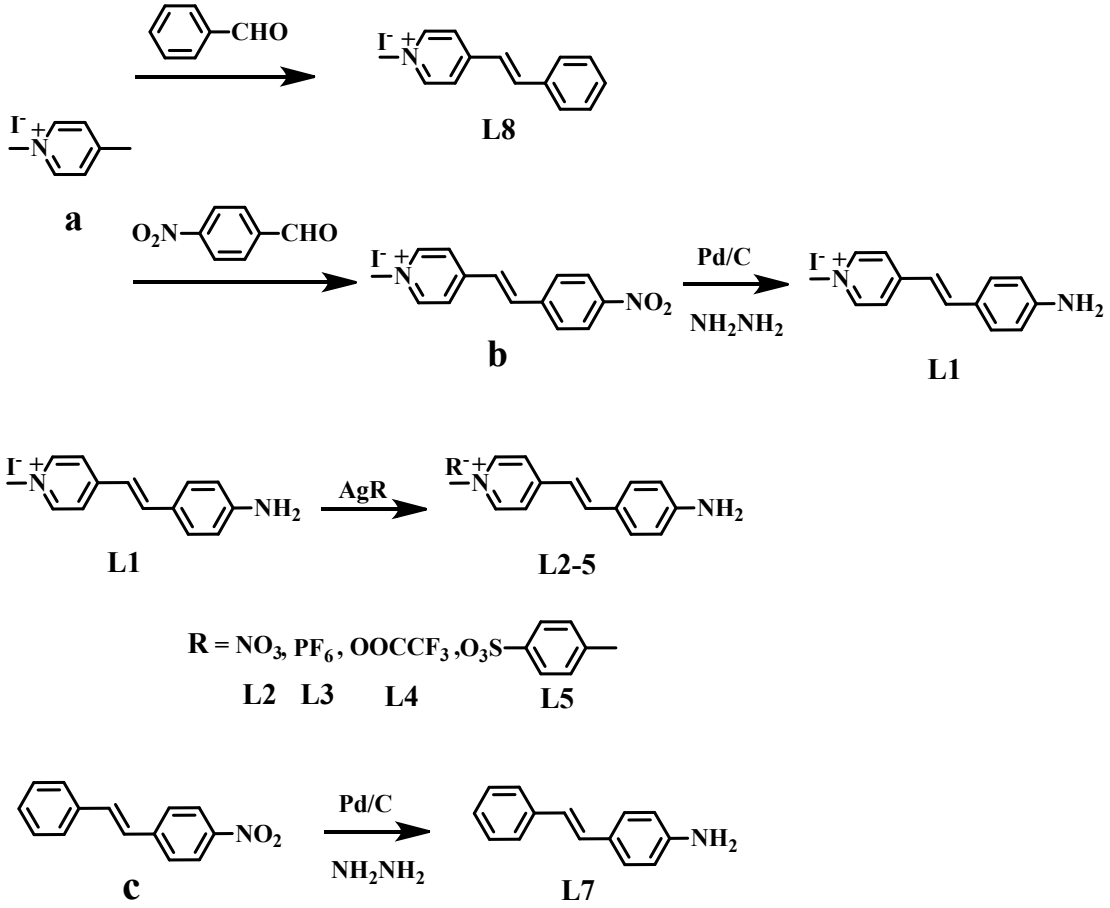

Scheme S1. Synthetic route for compounds **L1-8**.

1.1 Synthesis of **L1-8**

A series of new small weight **L1-8** were synthesized simply and facilely in high yield without tedious purification steps and outlined in **Scheme 1.** 1,4-dimethylpyridin-1-ium iodide **a**, (E)-1-methyl-4-(4-nitrostyryl)pyridin-1-ium iodide **b** and **L6** are synthesized efficiently according to the literature.[1,2] Benzaldehyde, 4-nitrobenzaldehyde, and (E)-1-nitro-4-styrylbenzene **c** are commercially available.

1,4-dimethylpyridin-1-ium iodide **a**: ^{1}H NMR (400 MHz, DMSO-d_6), δ (ppm): 8.89 (d, J = 6.00, 2H), 8.00 (d, J = 6.40, 2H), 4.33 (s, 3H), 2.62 (s, 3H). ^{13}C NMR (100 MHz, DMSO-d_6), δ (ppm): 158.17, 144.45, 127.94, 47.25, 21.39.

(E)-1-methyl-4-(4-nitrostyryl)pyridin-1-ium iodide **b**: ^{1}H NMR (400 MHz, DMSO-d_6), δ (ppm): 8.95 (d, J = 8.00, 2H), 8.35 (d, J = 8.00, 2H), 8.30 (d, J = 8.00, 2H), 8.13 (d, J = 16.00,

1H), 8.01 (d, J = 8.00, 2H), 7.77 (d, J = 16.00, 1H), 4.30 (s, 3H). ^{13}C NMR (100 MHz, DMSO-d_6), δ (ppm): 151.44, 147.73, 145.43, 141.51, 137.68, 128.97, 124.23, 124.17, 47.22.

1.1.1 Preparation of 4-(4-aminostyryl)-1-methylpyridin-1-ium iodide **L1**

0.70 g (368.17 g/mol, 1.90 mmol) of (E)-1-methyl-4-(4-nitrostyryl)pyridin-1-ium iodide **b** dissolved in 5 mL ethanol was added into a three-necked flask equipped with a magnetic stirrer and refluxed at 80 °C. Under the protection of nitrogen, 0.07g of Pd/C catalyst was added into the preceding reaction system and a solution of 2.5 mL of 85 % hydrazine hydrate dissolved in 10 mL ethanol was added dropwise for 0.5 h. The reaction was monitored by thin-layer chromatography (TLC). After the completion of the reaction, Pd/C catalyst filtered off and the solvent concentrated under reduced pressure, afforded **L1** as a red solid. Red solid was collected (0.53g, yield 82 %). ^{1}H NMR (400 MHz, DMSO-d_6), δ (ppm): 8.67 (d, J = 4.00 Hz, 2H), 8.01 (d, J = 8.00 Hz, 2H), 7.84 (d, J = 16.00 Hz, 1H), 7.46 (d, J = 8.00 Hz, 2H), 7.08 (d, J = 16.00 Hz, 1H), 6.62 (d, J = 8.00 Hz, 2H), 6.01 (s, 2H), 4.16 (s, 3H). ^{13}C NMR (100 MHz, DMSO-d_6) δ (ppm):153.45, 152.03, 144.26, 142.27, 130.47, 122.36, 121.95, 116.34, 113.73, 46.26. FT-IR (KBr, cm^{-1}) selected bands : 3287 (m), 3187 (m), 1585 (s), 1562 (m), 1517 (s), 1439 (w), 1298 (m), 975 (m), 837 (m). FTMS (+ESI): m/z 211.1226 (M^+, calcd *m/z* 211.1235), ITMS (-ESI): m/z 127 (I^-, calcd *m/z* 126.9050).

1.1.2 Preparation of 4-(4-aminostyryl)-1-methylpyridin-1-ium nitrate **L2**

4-(4-aminostyryl)-1-methylpyridin-1-ium iodide **L1** (0.10 g, 2.96×10^{-4} mol) was dissolved in 2 mL methanol and silver nitrate (0.05 g, 2.96×10^{-4} mol) was added into the preceding solution with vigorous stirring for 2 h at 50 °C. The mixture was then cooled, the precipitate filtered off, and the methanol was evaporated, red solid **L2** was obtained (80 mg, yield 93 %). ^{1}H NMR (400 MHz, DMSO-d_6), δ (ppm): 8.67 (d, J = 4.00 Hz, 2H), 8.01 (d, J = 8.00 Hz, 2H), 7.84 (d, J = 16.00 Hz, 1H), 7.46 (d, J = 8.00 Hz, 2H), 7.08 (d, J = 16.00 Hz, 1H), 6.62 (d, J = 8.00 Hz, 2H), 6.01 (s, 2H), 4.16 (s, 3H). ^{13}C NMR (100 MHz, DMSO-d_6), δ (ppm):153.45, 152.03, 144.26, 142.27, 130.47, 122.36, 121.95, 116.34, 113.73, 46.26. FT-IR (KBr, cm^{-1}) selected bands : 3325(m), 3187 (m), 1693 (s), 1558 (m), 1520 (s), 1443 (w), 1353 (m), 979 (m), 835 (m). MS (ESI): m/z 211.1226 (M^+, calcd *m/z* 211.1235).

1.1.3 Preparation of 4-(4-aminostyryl)-1-methylpyridin-1-ium hexafluorophosphate **L3**

4-(4-aminostyryl)-1-methylpyridin-1-ium iodide **L1** (0.10 g, 2.96×10^{-4} mol) was dissolved in 2 mL methanol, silver hexafluorophosphate (75 mg, 2.96×10^{-4} mol) was added into the preceding

solution with vigorous stirring for 2 h at 50 °C. The mixture was then cooled, the precipitate filtered off, and the methanol was evaporated, red solid **L3** was obtained (96 mg, yield 91 %). ^{1}H NMR (400 MHz, DMSO-d_6), δ (ppm):8.67 (d, J = 4.00 Hz, 2H), 8.01 (d, J = 8.00 Hz, 2H), 7.84 (d, J = 16.00 Hz, 1H), 7.46 (d, J = 8.00 Hz, 2H), 7.08 (d, J = 16.00 Hz, 1H), 6.62 (d, J = 8.00 Hz, 2H), 6.01 (s, 2H), 4.16 (s, 3H). ^{13}C NMR (100 MHz, DMSO-d_6) δ (ppm):153.46, 152.03, 144.26, 142.27, 130.47, 122.36, 121.95, 116.34, 113.73, 46.28. FT-IR (KBr, cm^{-1}): 3472 (m), 3391 (m), 1599 (s), 1568 (m), 1521 (s), 1441 (w), 1300 (m), 971 (m), 842 (m). FTMS (+ESI): m/z 211.1226 (M^+, calcd *m/z* 211.1235), ITMS (-ESI): m/z 145 (PF_6^-, calcd *m/z* 144.9642).

1.1.4 Preparation of 4-(4-aminostyryl)-1-methylpyridin-1-ium trifluoroacetate **L4**

4-(4-aminostyryl)-1-methylpyridin-1-ium iodide **L1** (0.10 g, 2.96×10^{-4} mol) was dissolved in 2 mL methanol and silver trifluoroacetate (65 mg, 2.96×10^{-4} mol) was added into the preceding solution with vigorous stirring for 2 h at 50 °C. The mixture was then cooled, the precipitate filtered off, and the methanol was evaporated, dark red solid **L4** was obtained (90 mg, yield 94 %). ^{1}H NMR (400 MHz, DMSO-d_6), δ (ppm): 8.67 (d, J = 4.00 Hz, 2H), 8.01 (d, J = 8.00 Hz, 2H), 7.84 (d, J = 16.00 Hz, 1H), 7.46 (d, J = 8.00 Hz, 2H), 7.08 (d, J = 16.00 Hz, 1H), 6.62 (d, J = 8.00 Hz, 2H), 6.01 (s, 2H), 4.16 (s, 3H). ^{13}C NMR (100 MHz, DMSO-d_6), δ (ppm):153.46, 152.04, 144.26, 142.28, 130.46, 129.68, 122.36, 121.95, 116.33, 113.41, 46.25. FT-IR (KBr, cm^{-1}): 3334 (m), 3187 (m), 1616 (m), 1592 (s), 1522 (s), 1446 (w), 1315 (m), 1171 (s), 1118 (s), 967 (m), 836 (m). FTMS (+ESI): m/z 211.1225 (M^+, calcd *m/z* 211.1235), ITMS (-ESI): m/z 113 ($^-OOCCF_3$, calcd *m/z* 112.9850).

1.1.5 Preparation of 4-(4-aminostyryl)-1-methylpyridin-1-ium toluenesulfonate **L5**

4-(4-aminostyryl)-1-methylpyridin-1-ium iodide **L1** (0.10 g, 2.96×10^{-4} mol) was dissolved in 5 mL methanol, silver p-toluenesulfonate (83 mg, 2.96×10^{-4} mol) was added into the preceding solution with vigorous stirring for 2 h at 50 °C. The mixture was then cooled, the precipitate filtered off, and the methanol was evaporated, dark red solid **L5** was obtained (103 mg, yield 91 %). ^{1}H NMR (400 MHz, DMSO-d_6), δ (ppm): 8.66 (d, J = 4.00 Hz, 2H), 8.01 (d, J = 8.00 Hz, 2H), 7.84 (d, J = 16.00 Hz, 1H), 7.46 (dd, J = 8.00 Hz, 4H), 7.10 (m, 3H), 6.62 (d, J = 8.00 Hz, 2H), 6.01 (s, 2H), 4.16 (s, 3H), 2.28 (s, 3H). ^{13}C NMR (100 MHz, DMSO-d_6), δ (ppm):153.45, 152.03, 145.83, 144.26, 142.27, 137.48, 130.47, 127.99,125.45, 122.36, 121.95, 116.34, 113.73, 46.28, 20.74. FT-IR (KBr, cm^{-1}) selected bands: 3342 (m), 3214 (m), 1603 (s), 1563 (m), 1521 (s), 1446

(w), 1312 (m), 1191 (s), 1123 (s), 971 (m), 838 (m). FTMS (+ESI): m/z 211.1224 (M^+, calcd *m/z* 211.1235), ITMS (-ESI): m/z 171 ($C_7H_7SO_3^-$, calcd *m/z* 171.0116).

1.1.6 Preparation of (E)-4-(2-(pyridin-4-yl)vinyl)aniline **L6**

The probe L6 is synthesized efficiently according to the literature.[3,4] ^{1}H NMR (400 MHz, DMSO-d_6), δ (ppm): 8.46 (d, J = 4.00, 2H), 7.44 (d, J = 8.00, 2H), 7.33-7.37 (m, 3H), 6.86 (d, J = 16.00, 1H), 6.58 (d, J = 8.00, 2H), 5.51 (s, 2H). ^{13}C NMR (100 MHz, DMSO-d_6), δ (ppm): 149.77, 149.72, 145.27, 133.76, 128.47, 123.59, 120.15, 119.77, 113.74. FT-IR (KBr, cm^{-1}) selected bands: 3318 (m), 3185 (m), 1626 (m), 1584 (s), 1516 (s), 1414 (w), 1312 (s), 971 (s), 827 (s), MS (APCI): m/*z* 197.1073 ([M+H]$^+$, calcd m/*z* 197.1079).

1.1.7 Preparation of (E)-1-methyl-4-styrylpyridin-1-ium iodide **L7**

0.30 g (225.24 g/mol, 1.33 mmol) of (E)-1-nitro-4-styrylbenzene **c** dissolved in 5 mL ethanol was added into a three-necked flask equipped with a magnetic stirrer and refluxed at 80 °C. Under the protection of nitrogen, 0.03 g of Pd/C catalyst was added into the preceding reaction system and a solution of 1 mL of 85 % hydrazine hydrate dissolved in 5 mL ethanol was added dropwise for 0.5 h. The reaction was monitored by TLC. After the completion of the reaction, Pd/C catalyst filtered off and concentrated under reduced pressure to provide white solid. White solid **L7** was collected (0.21 g, yield 81 %). ^{1}H NMR (400 MHz, DMSO-d_6, ppm) δ:7.49 (d, J = 8.00 Hz, 2H), 7.34-7.27 (m, 4H), 7.18 (t, J = 8.00 Hz, 1H), 7.06 (d, J = 16.00 Hz, 1H), 6.89 (d, J = 16.00 Hz, 1H), 6.56 (d, J = 8.00 Hz, 2H), 5.32 (s, 2H), ^{13}C NMR (100 MHz, DMSO-d_6, ppm) δ:148.76, 137.93, 129.07, 128.56, 127.61, 125.68, 124.61, 122.67, 113.82. FT-IR (KBr, cm^{-1}) selected bands: 3447 (m), 3361 (m), 1615 (m), 1588 (m), 1517 (s), 1446 (w), 970 (s), 818 (s). MS (ESI): m/z 196.1120 ([M+H]$^+$, calcd *m/z* 196.1126).

1.1.8 Preparation of 1-methyl-4-styrylpyridin-1-ium iodide **L8**

0.50g (235.06 g/mol, 2.13 mmol) of **a**, 0.23 g (106.12 g/mol, 2.13 mmol) of benzaldehyde, and 5 mL ethanol were mixed. Five drops of piperidine were added to the mixture. Then the solution refluxed at 70 °C for 6 h, cooled and a dark yellow solid formed and filtered. The solid was washed twice with ethanol. Yellow solid was collected (0.59 g, yield 86 %). ^{1}H NMR (400 MHz, DMSO-d_6, ppm), δ: 8.87 (d, J = 4.00, 2H), 8.23 (d, J = 8.00, 2H), 8.01 (d, J = 16.00, 1H), 7.76 (d, J = 8.00, 2H), 7.55-7.46 (m, 4H), 4.26 (s, 3H). ^{13}C NMR (100 MHz, DMSO-d_6, ppm), δ: 152.41, 145.11, 140.55, 135.11, 130.36, 129.10, 128.06, 123.56, 123.28, 49.93. FT-IR

(KBr ,cm^{-1}) selected bands: 3023 (m), 1642 (m), 1626 (s), 1518 (s), 1473 (w), 973 (m), 838 (m). MS (ESI): m/z 196.1120 (M^+, calcd m/z 196.1126).

1.2 Materials and apparatus

All chemicals and reagents were obtained commercially and used without further purification. The samples were detected at room temperature immediately in water solution. The ^1H NMR and ^{13}C NMR spectra were measured on a Bruker Avance spectrometer using DMSO-d_6 or D_2O as the solvents (400 MHz for ^1H NMR and 100 MHz for ^{13}C NMR). STD NMR experiments were performed on a 700 MHz Bruker spectrometer equipped with a triple resonance cryoprobe. The mass spectra were obtained on a Thermo Fisher Scientific LTQ-Orbitrap mass spectrometer. IR spectra were recorded with a Nicolet FT-IR NEXUS 870 spectrometer (KBr discs) in the 4000-400 cm^{-1} region. One-photon absorption (OPA) spectra were recorded on a UV-265 spectrophotometer. One-photon excited fluorescence (OPEF) spectra were performed using a Hitachi F-7000 fluorescence spectrophotometer. Two-photon emission fluorescence (TPEF) spectra were measured at femtosecond laser pulse and Ti: sapphire system (680–1080 nm, 80 MHz, 140 fs) as the light source.

1.3 Two-photon action cross-section

Two-photon (TP) action cross-sections of all compounds were obtained by the two-photon excited fluorescence (TPEF) method with femtosecond laser piles and a Ti: sapphire system (680-1080 nm, 80 MHz, 140 fs) as the light source. Two-photon action cross-section ($\sigma\Phi$) values were determined by the following equation:

$$\sigma\Phi = \sigma_{ref}\Phi_{ref}\frac{c_{ref}}{c}\frac{n_{ref}}{n}\frac{F}{F_{ref}}$$

Here, the subscripts *ref* stands for the reference molecule (Rhodamine 6G). Φ is the quantum yield, n is the refractive index, F is the integrated area under the corrected emission spectrum, c is the concentration of the solution in $mol \cdot L^{-1}$. The σ_{ref} value of reference was taken from the literature.[5] The two-photon induced fluorescence spectra of the reference and sample emitted at the same excitation wavelength were determined.

1.4 General UV–Vis, fluorescence and STD NMR spectra measurements

Stock solutions (1 mL) of the S. cerevisiae RNA (RNA), Calf Thymus DNA (DNA), bovine serum albumin (BSA) and phosphatidylcholine (PC) were prepared in Tris-HCl (pH = 7.4) buffer.

Stock solution of L1-8 (1 mM) were prepared in distilled water. Test solutions were prepared by placing 50 μL of the compound stock solution into a test tube, adding an appropriate aliquot of RNA, DNA, BSA, and PC, and diluting the solution to 5 mL with Tris- HCl (pH = 7.4) buffer. One-photon absorption (OPA) and excited fluorescence (OPEF) spectra, two-photon emission fluorescence (TPEF) spectra were obtained in Tris- HCl (pH = 7.4) buffer. 50 μM RNA was dissolved in 0.5 mL of 20 mM phosphate-buffered H_2O/D_2O 1:1, adjusted to pH 6.8, containing 50 mM NaCl. Temperature was set to 10 °C, 256 scans were acquired for the STD spectrum, and STD NMR spectrum of the mixture with on-resonance irradiation at 15.5 ppm and a saturation time of 5 s. A G4 Gaussian cascade pulse of 20 ms with an excitation bandwidth of ca. 0.8 ppm was used. A single Gaussian pulse of the same duration has an excitation profile of ca. 0.2 ppm.

1.5 Microscopy and micrographs analysis

HeLa cells were luminescently imaged on a Zeiss LSM 710 META upright confocal laser-scanning microscope. An incubation chamber was applied for live-cell and Real-Time (RT) imaging, which was connected to temperature control unit 37°C and CO_2 controller (1-2 hours before the experiment was allowed for stabilization of the temperature and CO_2 concentration). Quantification of the micrographs fluorescence intensity was done *via* an ImageJ plug-in ROI (region of interesting) manager. At least three micrographs for each experiment are required, and 10 data points from each micrograph are obtained. The acquisition of co-localisation data by means of Pearson's correlation coefficient was done via an ImageJ plug-in 'Colocalization Finder' (Dye A = yellow, Dye B = red. Rr (-1< Rr <1) refers to the Pearson correlation coefficient, where: Rr = 1 = perfect colocalization; Rr = 0 = random localization; Rr = -1 = perfect exclus

1.6 Cytotoxicity test

The effect of L1-8 on viability of cells were carried out using the methylthiazolyldiphenyl-tetrazolium bromide (MTT) assay. HeLa cells were cultured in a 96-well plate for 24h before experiments. The cell medium was then exchanged by different concentrations of L1-8 medium solutions (5, 10, 15, 20, 25 μM). They were then incubated at 37 °C in 5% CO_2 for 24 h before cell viability was measured by the MTT assay. The cell medium solutions were exchanged by 100 μL of fresh medium, followed by the addition of 10 μL (5 mg/mL) MTT solution to each well. The cell plates were then incubated at 37 °C in 5% CO_2 for 24 h. Absorbance was measured at 570 nm. The absorbance measured for an untreated cell population under the same experimental

conditions was used as the reference point to establish 100% cell viability. Duplicated experiments have been tested.

1.7 Cell culture and co-staining

HeLa cells were grown in the medium which was Dulbecco's modified Eagle's medium (DMEM) supplemented with 10% fetal calf serum (FCS, GIBCO), fungizone and L-glutamine, streptomycin and penicillin. For live cell confocal laser scanning microscopy experiment, HeLa cells were seeded in 24-well glass bottom plate at density of 10,000, and incubated for 72-96 hours at 37 °C in 95% air 5% CO_2 in order to allow the cells to reach ~90% confluence, the medium changed every two days. Compounds L1-8 (1 mM) were prepared in DMSO solution, and diluted in culture medium at 10 μM for 30 min at 37 °C in 95% air 5% CO_2 and then imaged with confocal microscopy. Syto-RNA select (Syto-9) ，Mito-Tracker Deep Red (Mito-deepred)，ER-Tracker Red (ER-Red) and CellMask Deep Red (CellMask) were dissolved in DMSO at a concentration of 1 mM and DAPI was prepared as 1 mM aqueous solution. Syto-9 (λex = 488 nm, λem = 501 nm) was a membrane-permeable nucleic acid dye, which only stains the live cells RNA contents. Mito-Tracker deep red (λex = 644 nm, λem = 665 nm) was a commercial mitochondrial dye. DAPI (λex = 340 nm, λem = 488 nm) was a DNA-specific dye. ER-red (λex = 587 nm, λem = 615 nm) was used for live-cell endoplasmic reticulum labeling. The CellMask Deep Red (λex = 650 nm, λem = 655 nm) allowed fast and uniform labeling of the plasma membrane.

For colocalization experiments, L1-5 (10 μM) was incubated with HeLa cells in DMEM for 30 min, and then the medium were replaced with fresh medium in the presence of Mito-Tracker Deep Red dye (1 μM), Syto-9 (1 μM) , DAPI (1 μM) , ER-red (1 μM) or CellMask Deep Red (1 μM) for 20 min. The 24-well plate were washed thrice by PBS and imaged. In the DNase digest test, only DNA substrates were hydrolyzed in the cells while in the RNase digest test, only RNA substrates were hydrolyzed. Carbonyl cyanide m-chlorophenylhydrazone (CCCP) can collapsed mitochondrial membrane potential. Mito-deep red, whose uptake was dependent on the mitochondria membrane potential, was inconsistent in the absence or presence of CCCP.

1.8 Photostability of L1-5

Photostability of fluorescent probes was a vital factor for biological applications. We used laser irradiation to scan persistently the stained cells to quantitatively investigate the photobleaching resistance of L1-5, Mito-Tracker deep red and Syto-9, and the fluorescent signals

were obtained over time (Fig. S43, S44), indicating that the prepared L1-5 possessed better photostability than Mito-Tracker deep red and Syto-9.

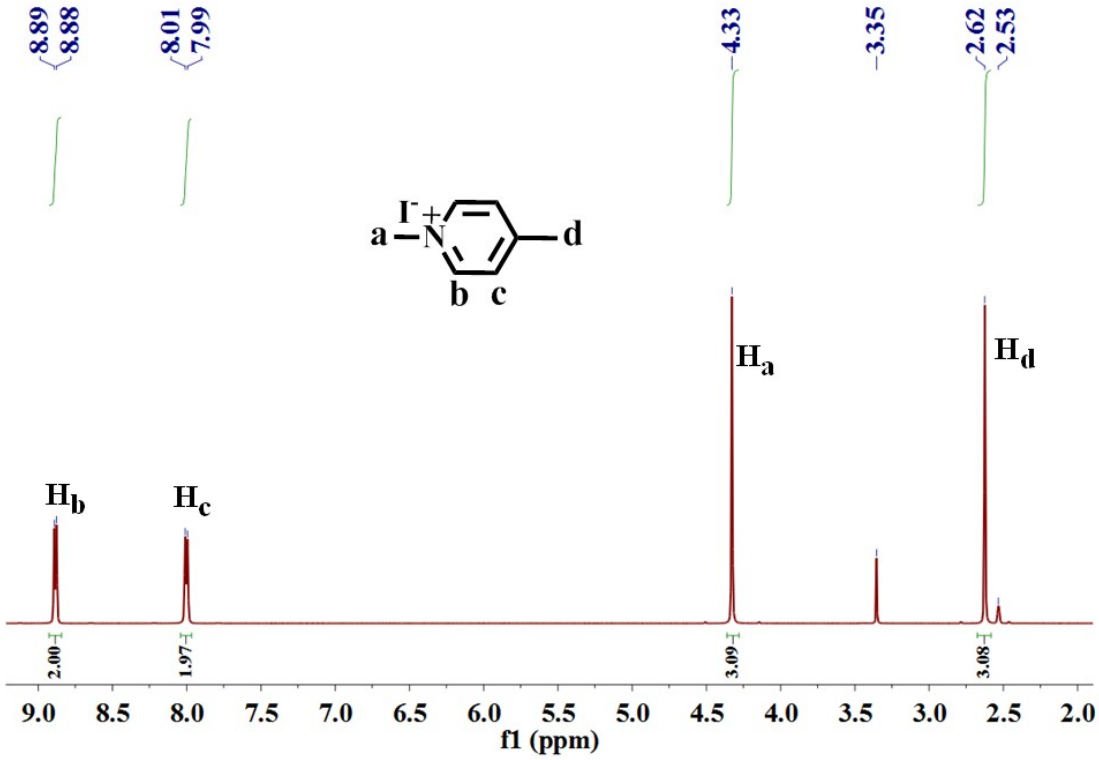

Fig. S1: ^{1}H NMR spectrum of a (DMSO-d_6)

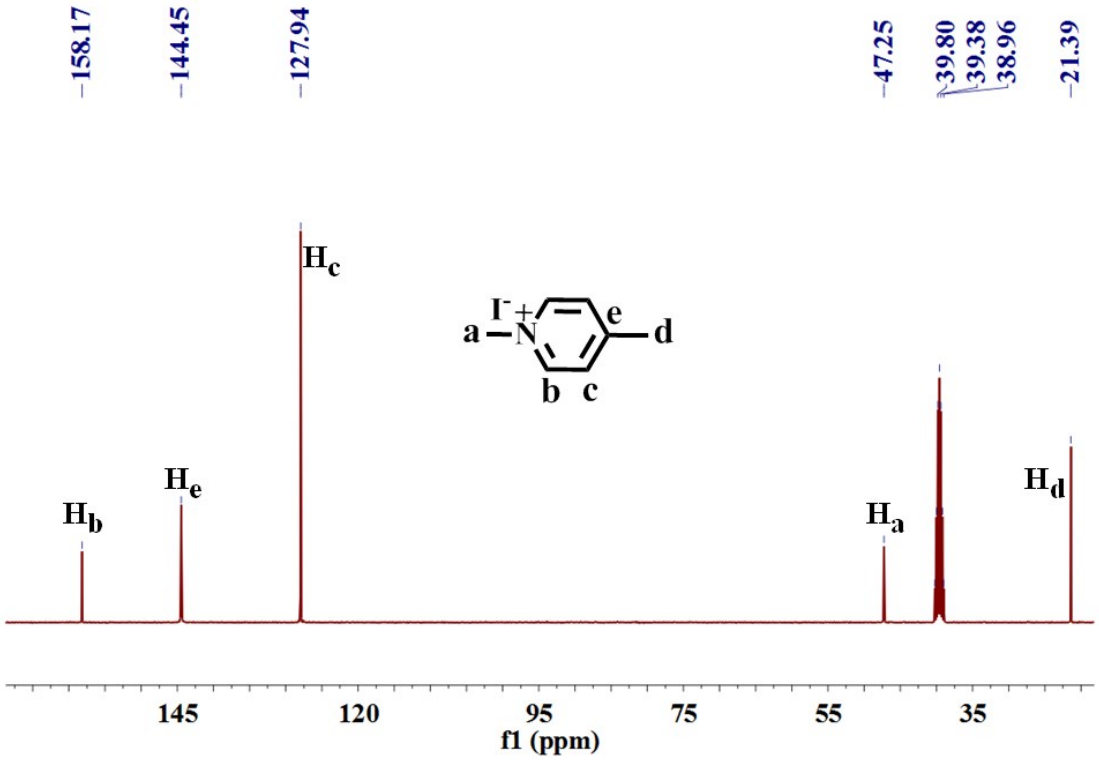

Fig. S2: ^{13}C NMR spectrum of a (DMSO-d_6)

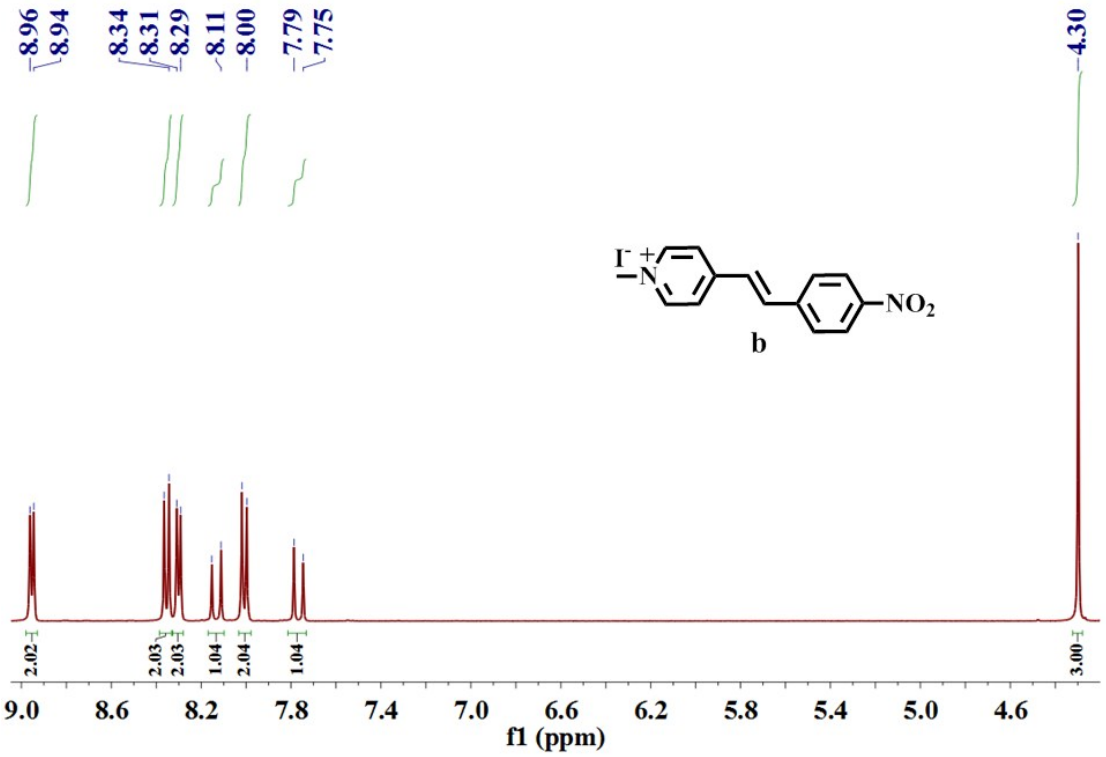

Fig. S3: ^{1}H NMR spectrum of b (DMSO-d_6)

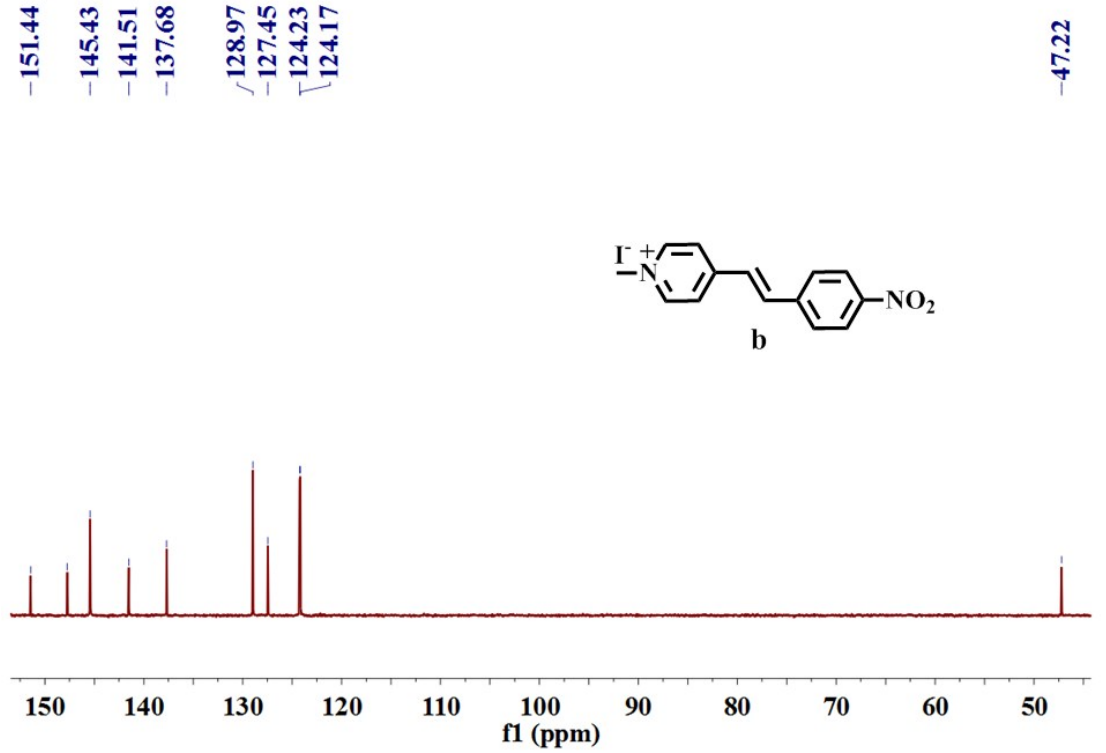

Fig. S4: ^{13}C NMR spectrum of b (DMSO-d_6)

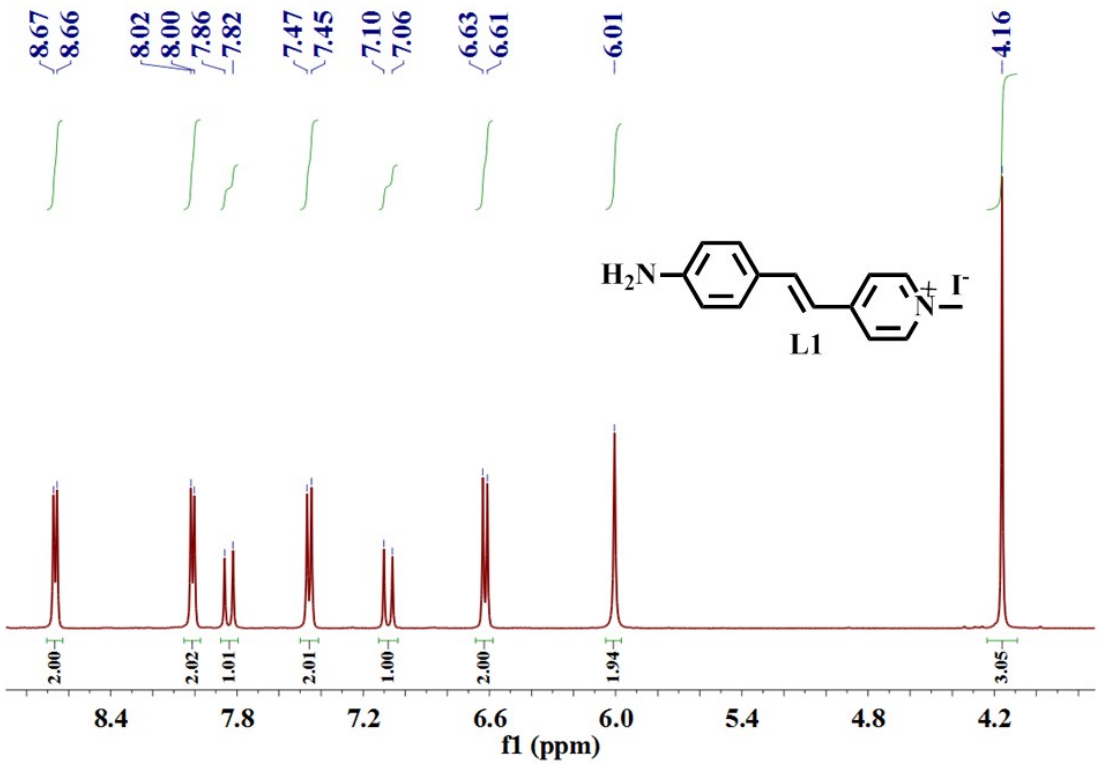

Fig. S5: ^{1}H NMR spectrum of L1 (DMSO-d_6)

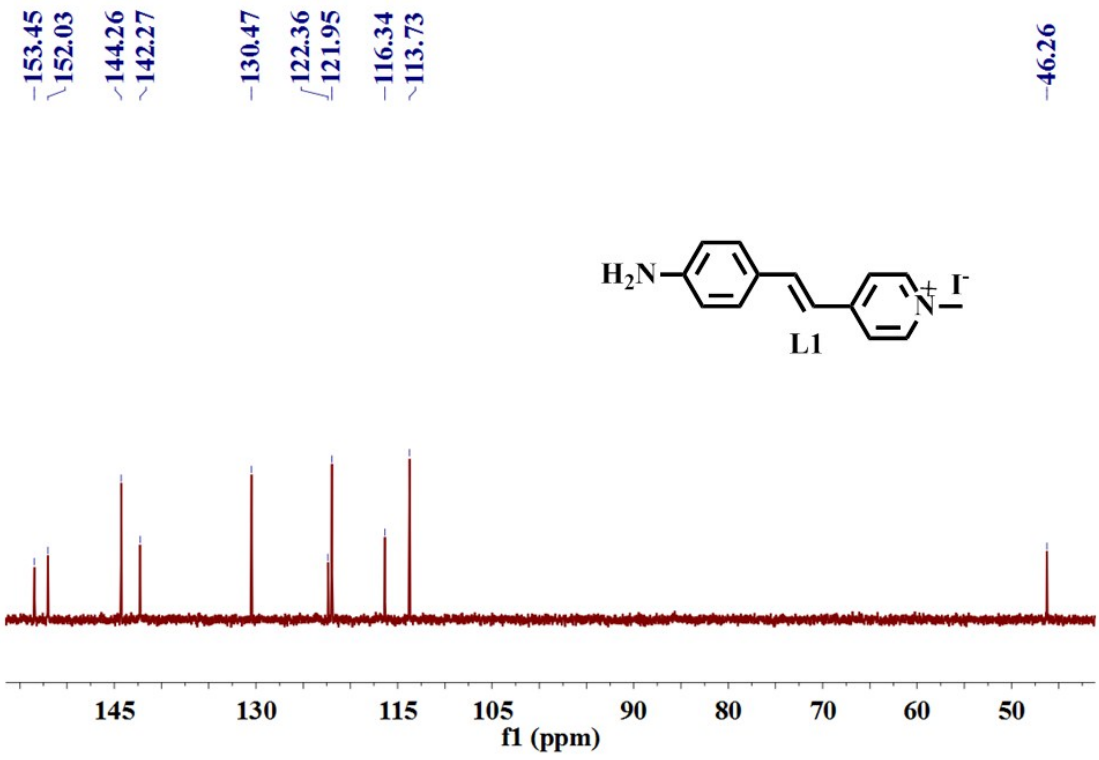

Fig. S6: ^{13}C NMR spectrum of L1 (DMSO-d_6)

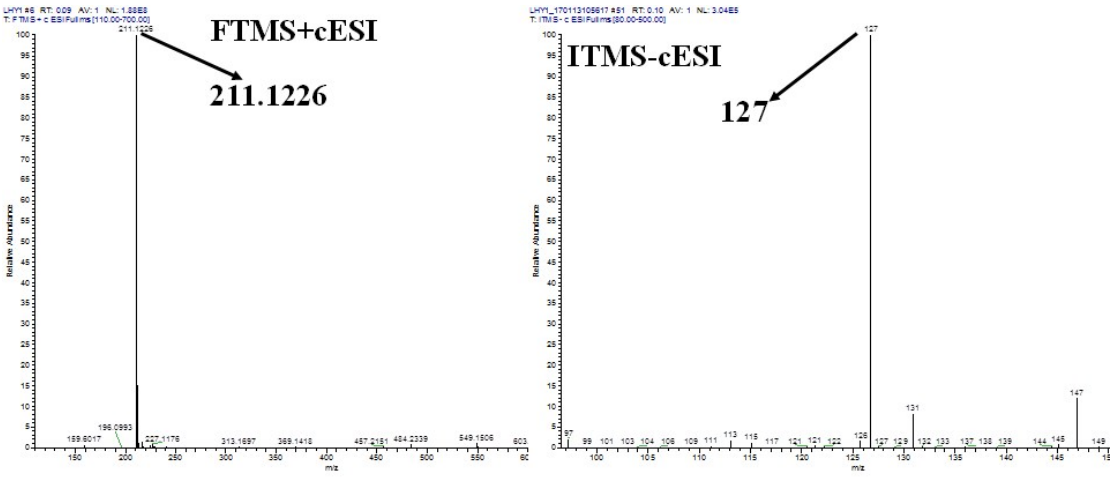

Fig. S7: ESI-Mass spectrum of L1

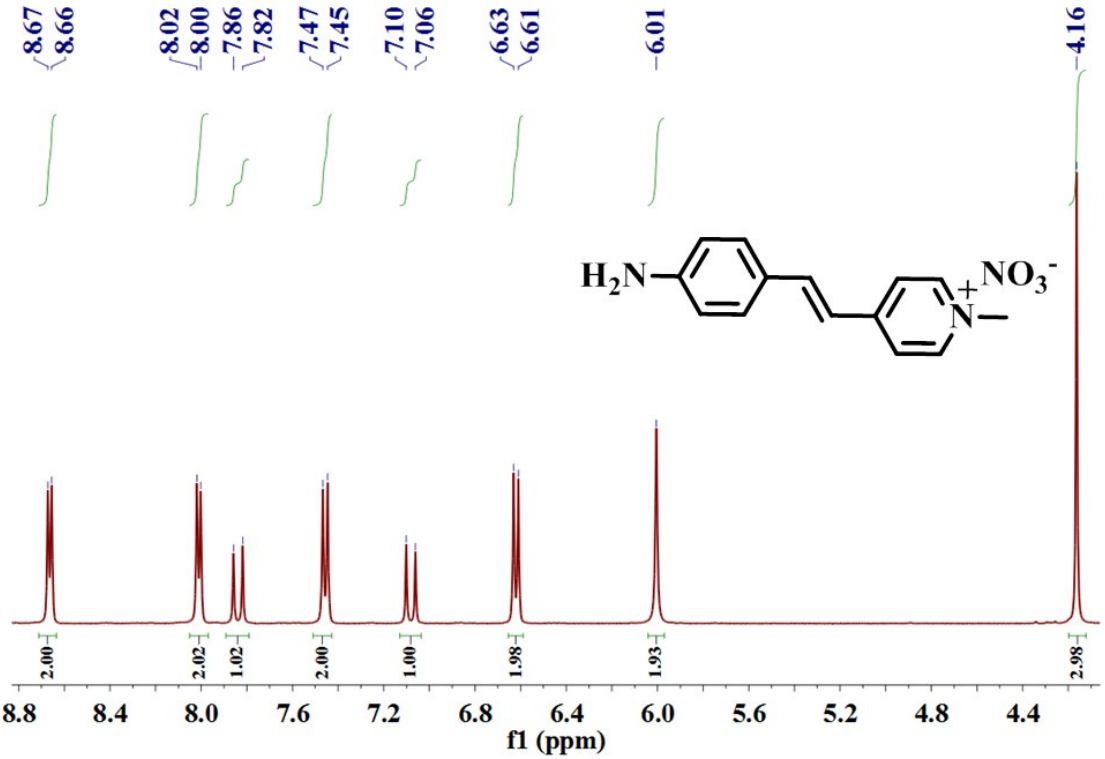

Fig. S8: ^{1}H NMR spectrum of L2 (DMSO-d_6)

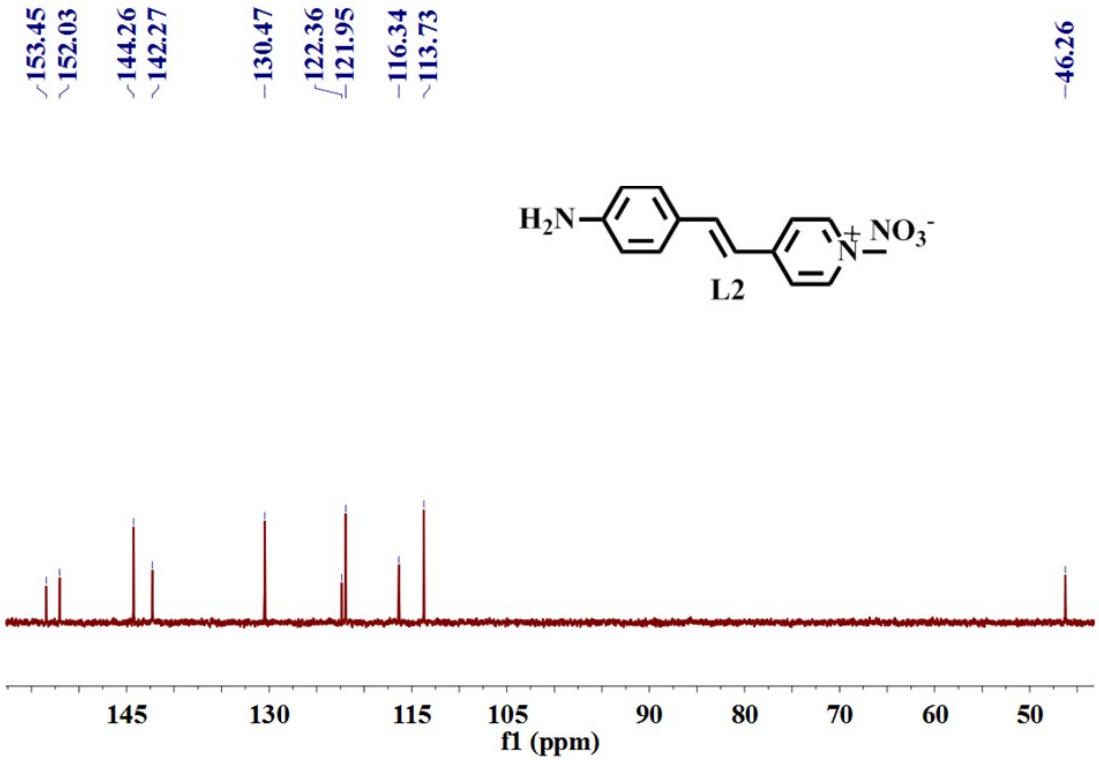

Fig. S9: ^{13}C NMR spectrum of L2 (DMSO-d_6)

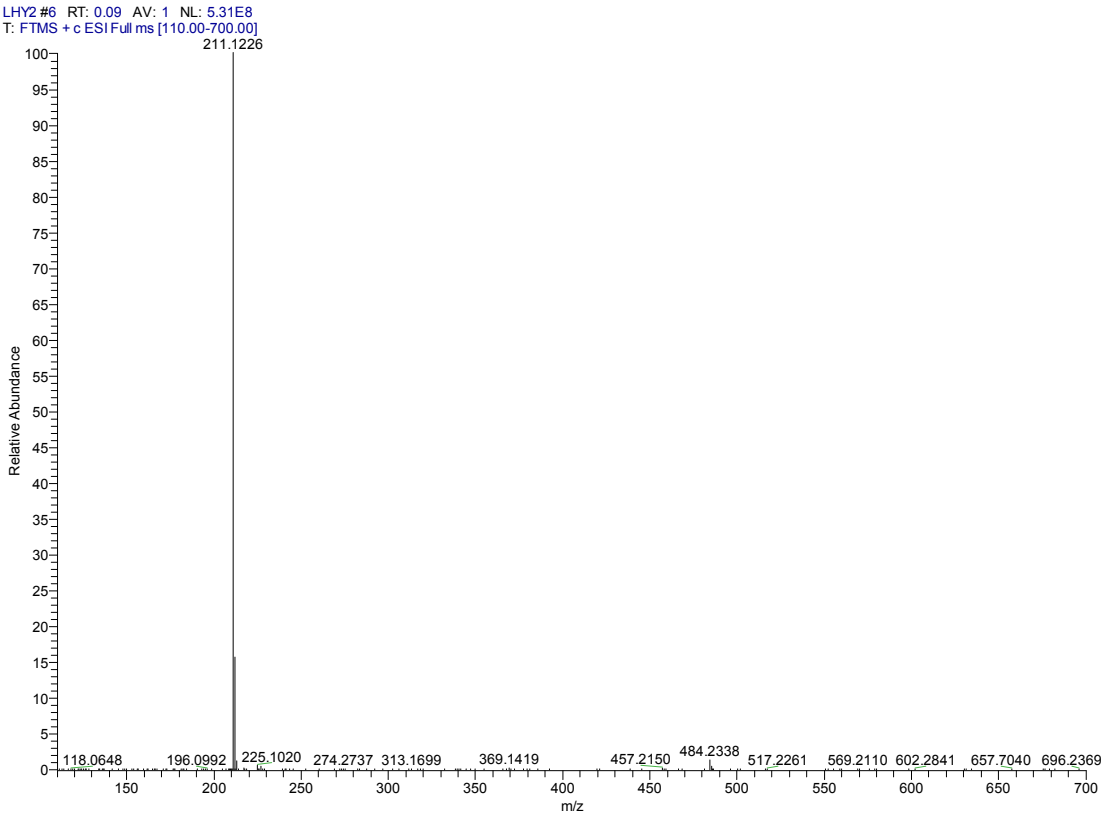

Fig. S10: ESI-Mass spectrum of L2

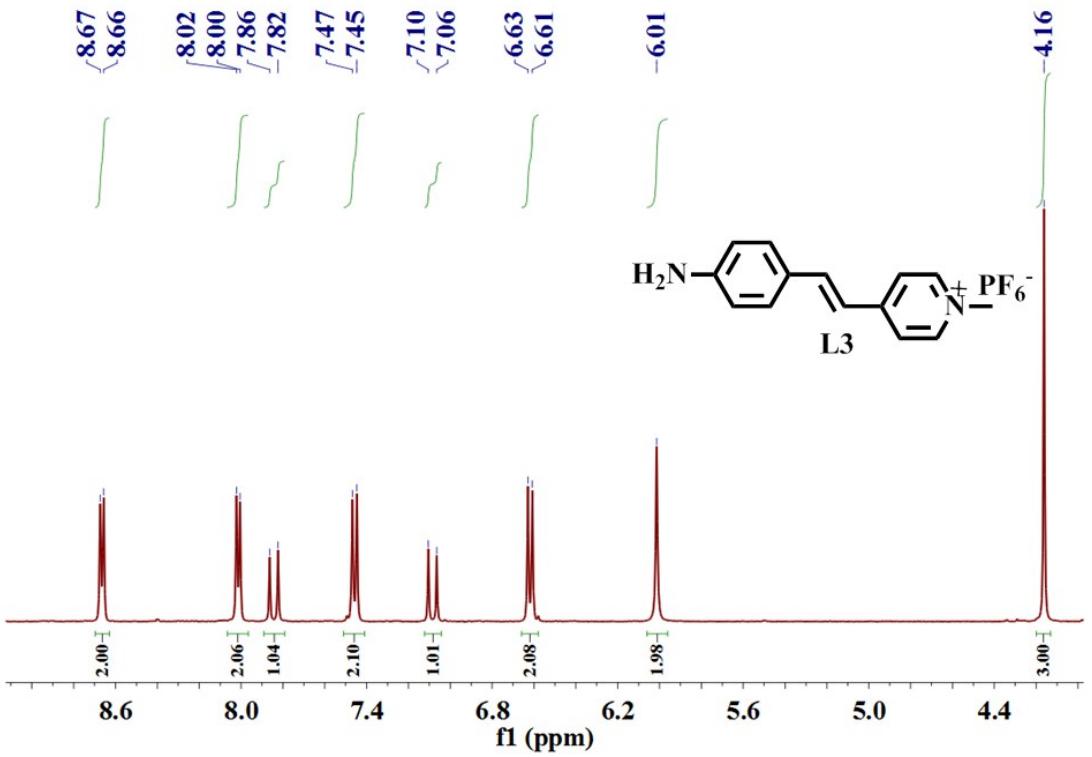

Fig. S11: ^{1}H NMR spectrum of L3 (DMSO-d_6)

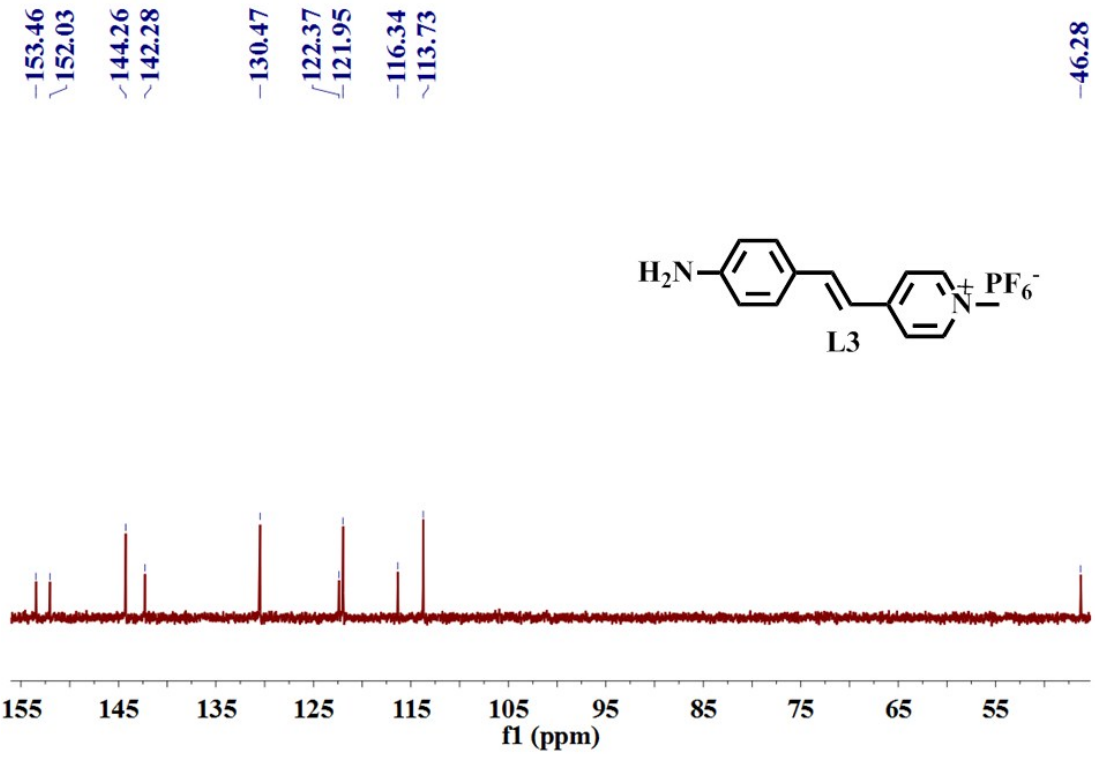

Fig. S12: ^{13}C NMR spectrum of L3 (DMSO-d_6)

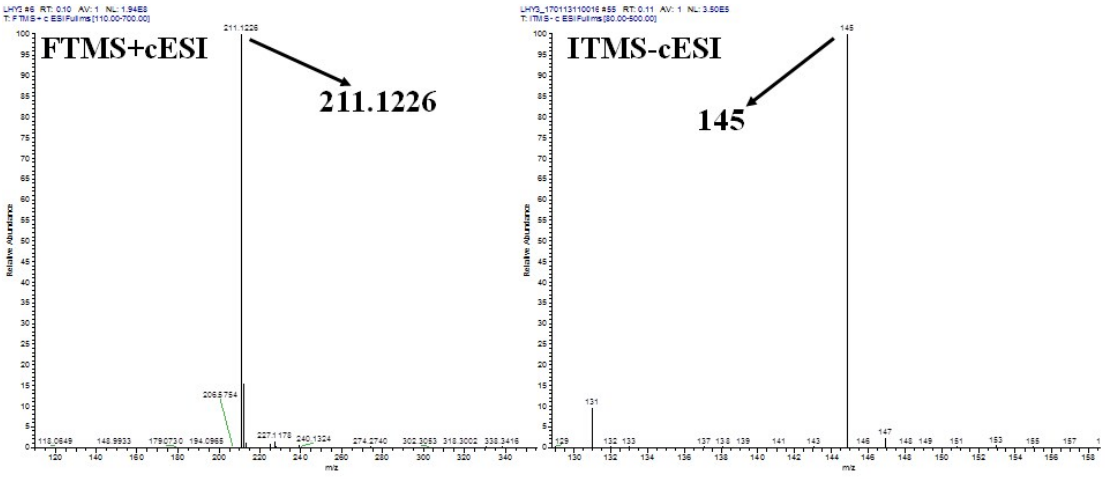

Fig. S13: ESI-Mass spectrum of L3

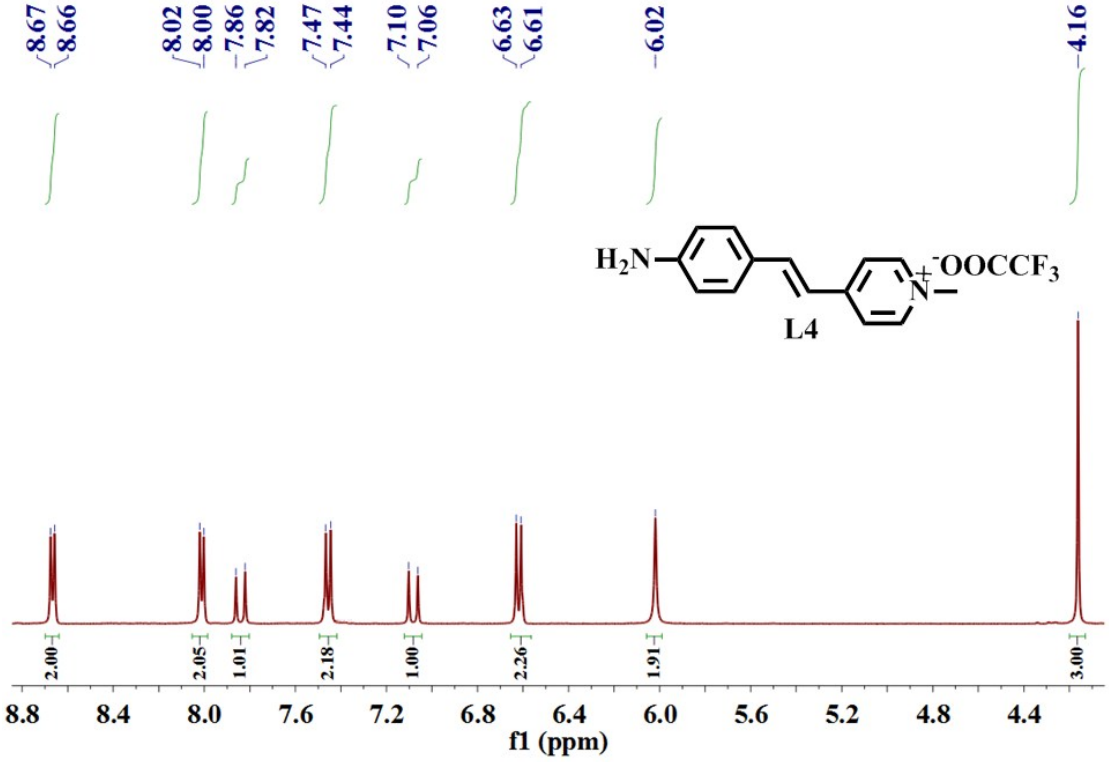

Fig. S14: ^{1}H NMR spectrum of L4 (DMSO-d_6)

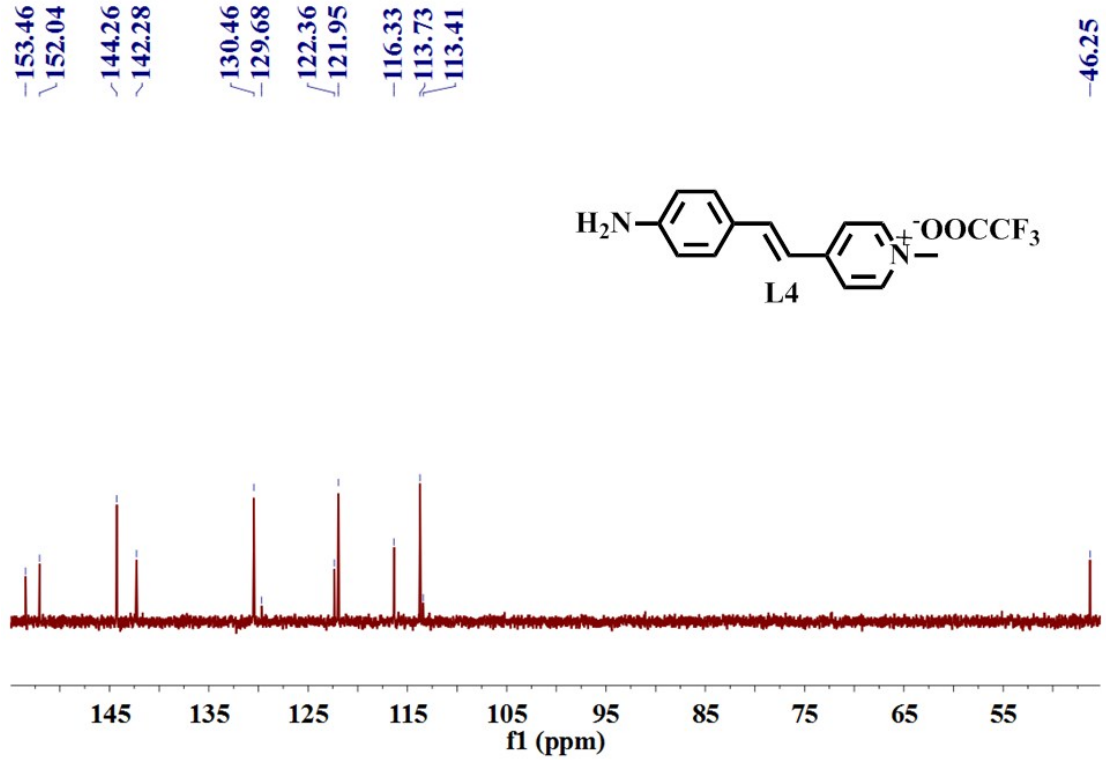

Fig. S15: ^{13}C NMR spectrum of L4 (DMSO-d_6)

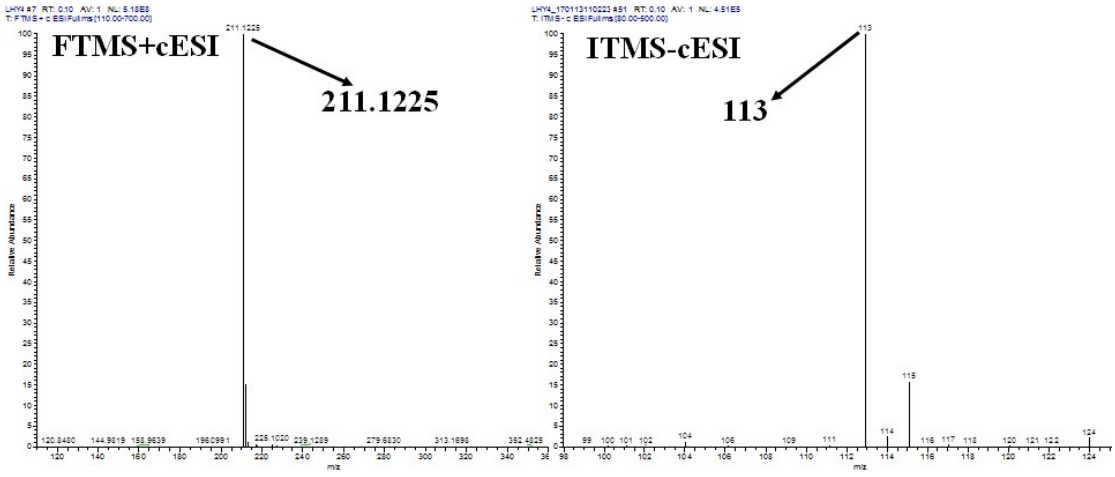

Fig. S16: ESI-Mass spectrum of L4

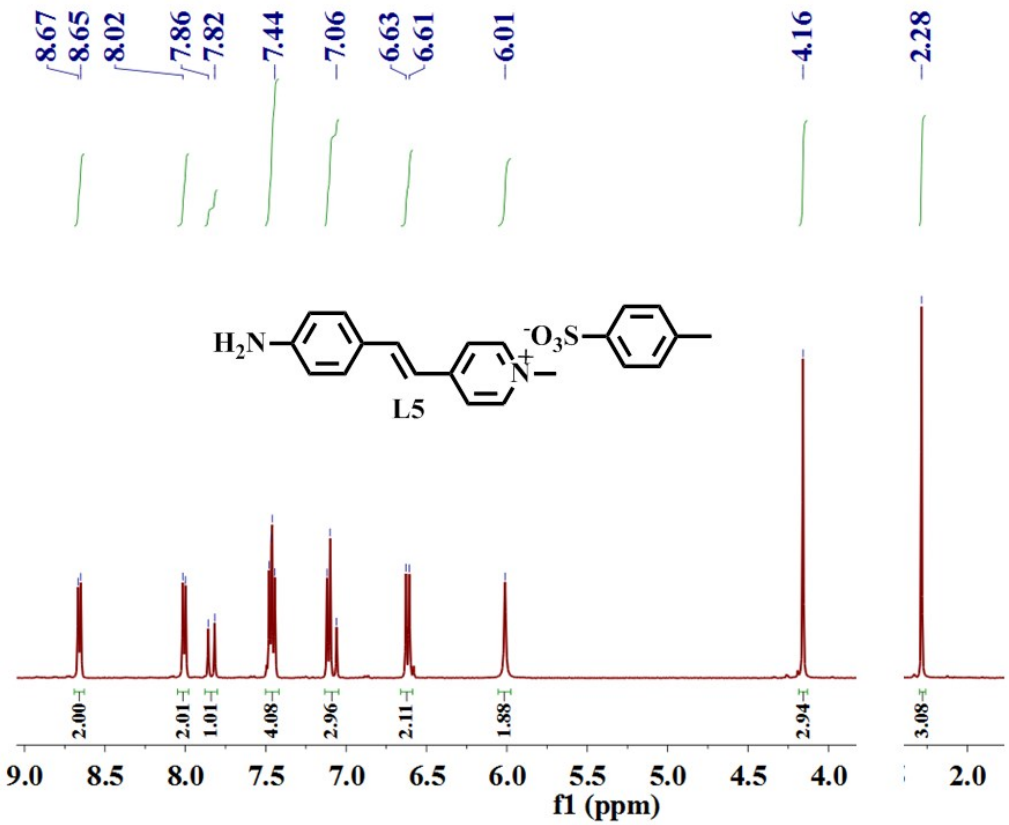

Fig. S17: [1]H NMR spectrum of L5 (DMSO-d_6)

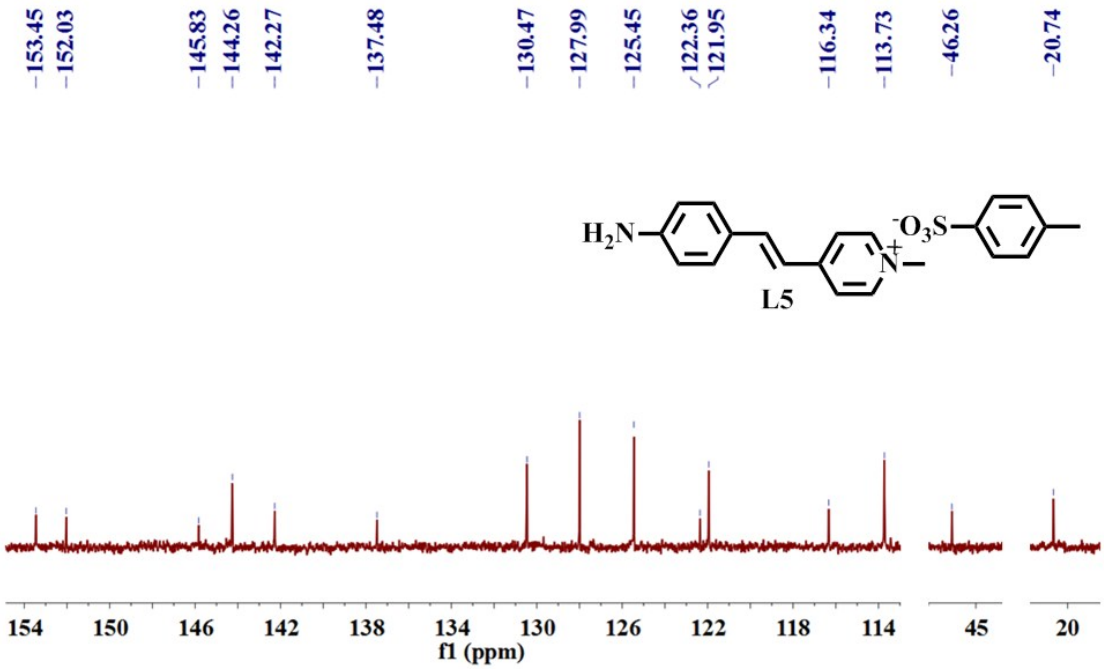

Fig. S18: [13]C NMR spectrum of L5 (DMSO-d_6)

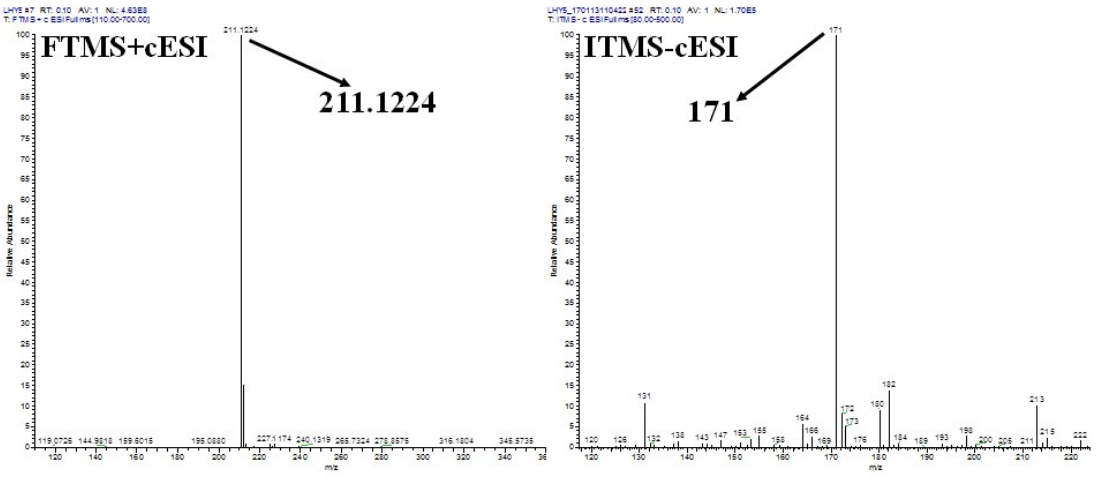

Fig. S19: ESI-Mass spectrum of L5

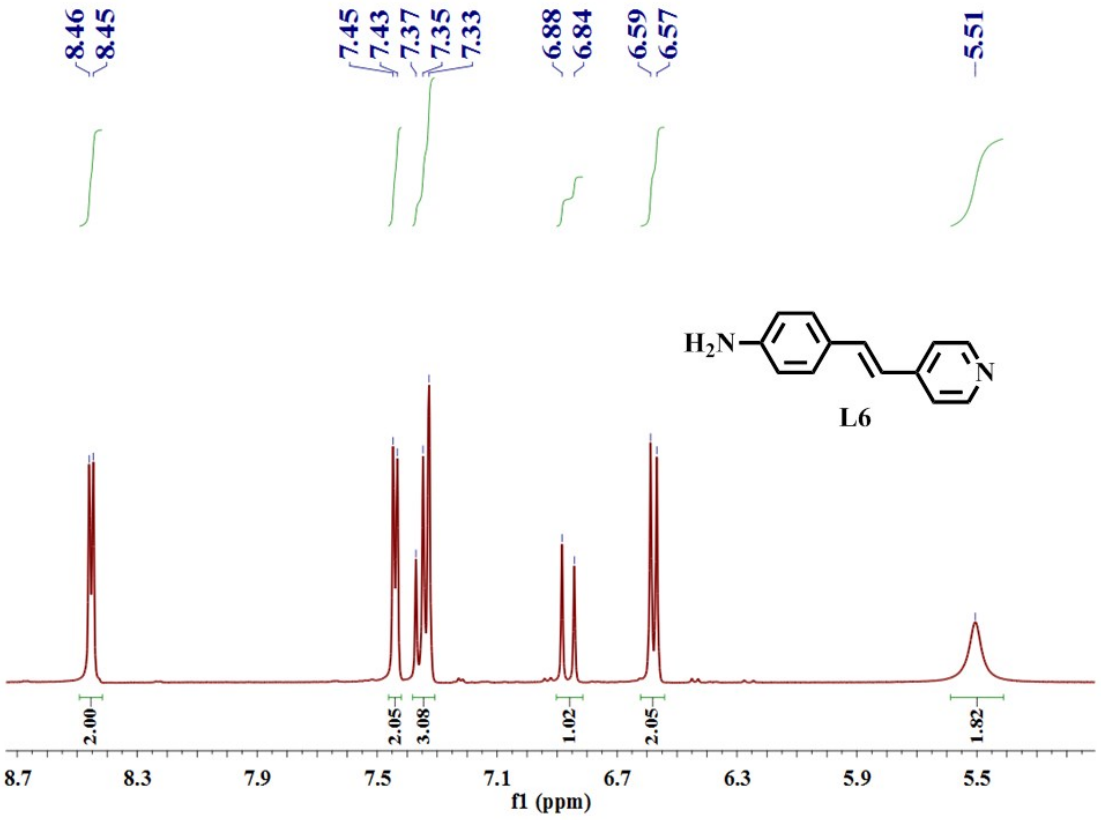

Fig. S20: ^{1}H NMR spectrum of L6 (DMSO-d_6)

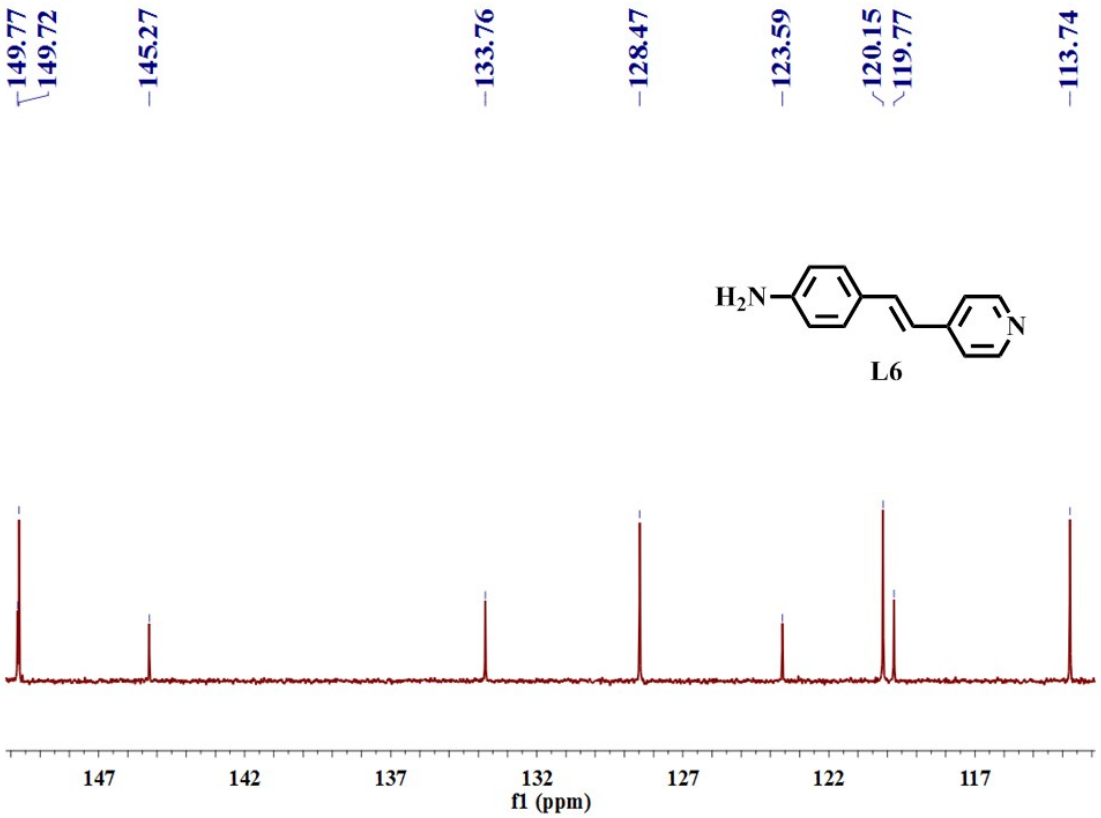

Fig. S21: ^{13}C NMR spectrum of L6 (DMSO-d_6)

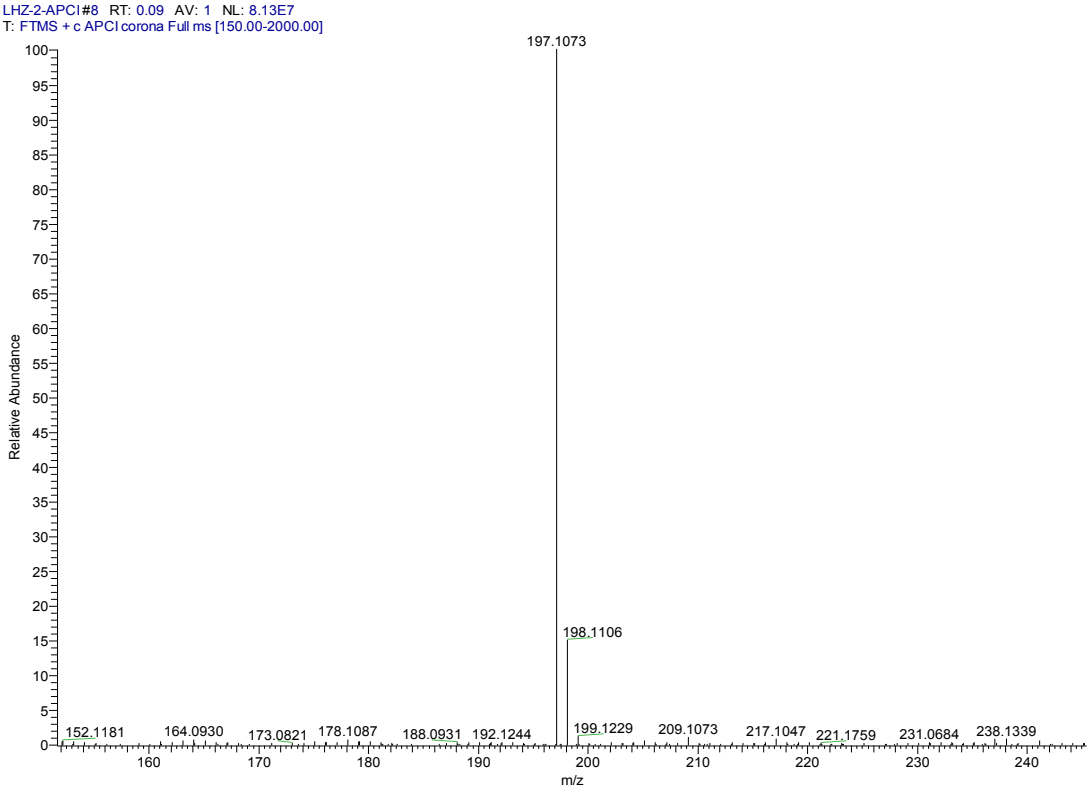

Fig. S22: APCI-Mass spectrum of L6

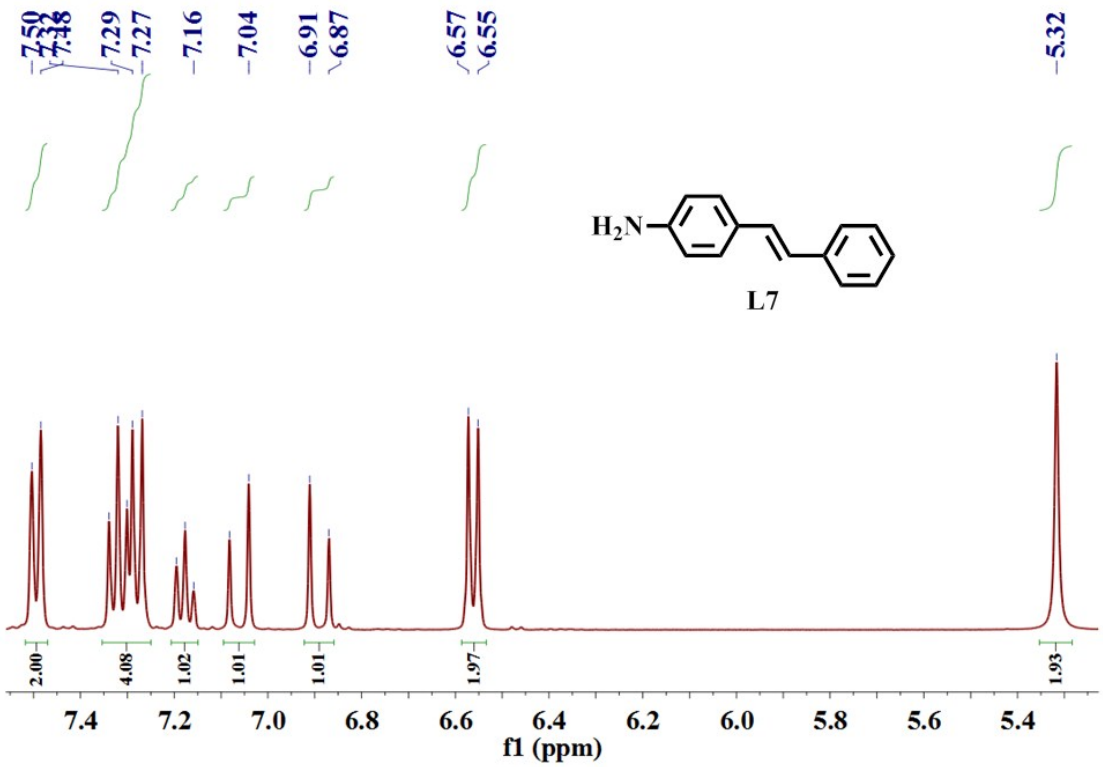

Fig. S23: ^{1}H NMR spectrum of L7 (DMSO-d_6)

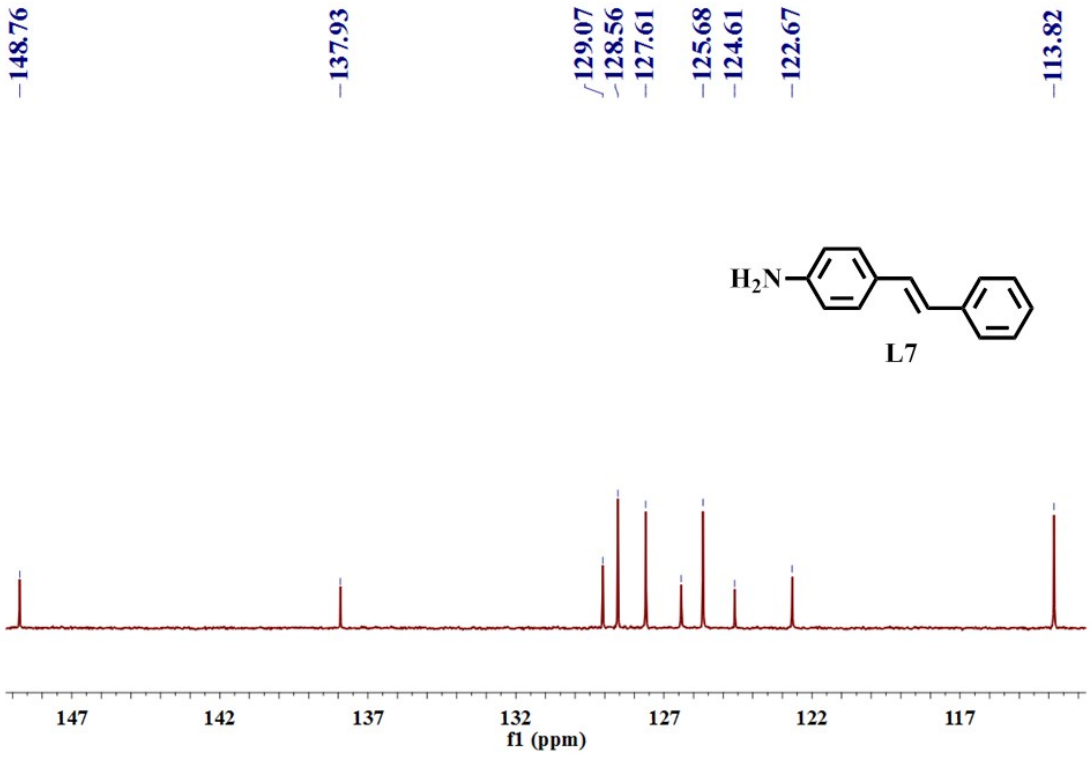

Fig. S24: ^{13}C NMR spectrum of L7 (DMSO-d_6)

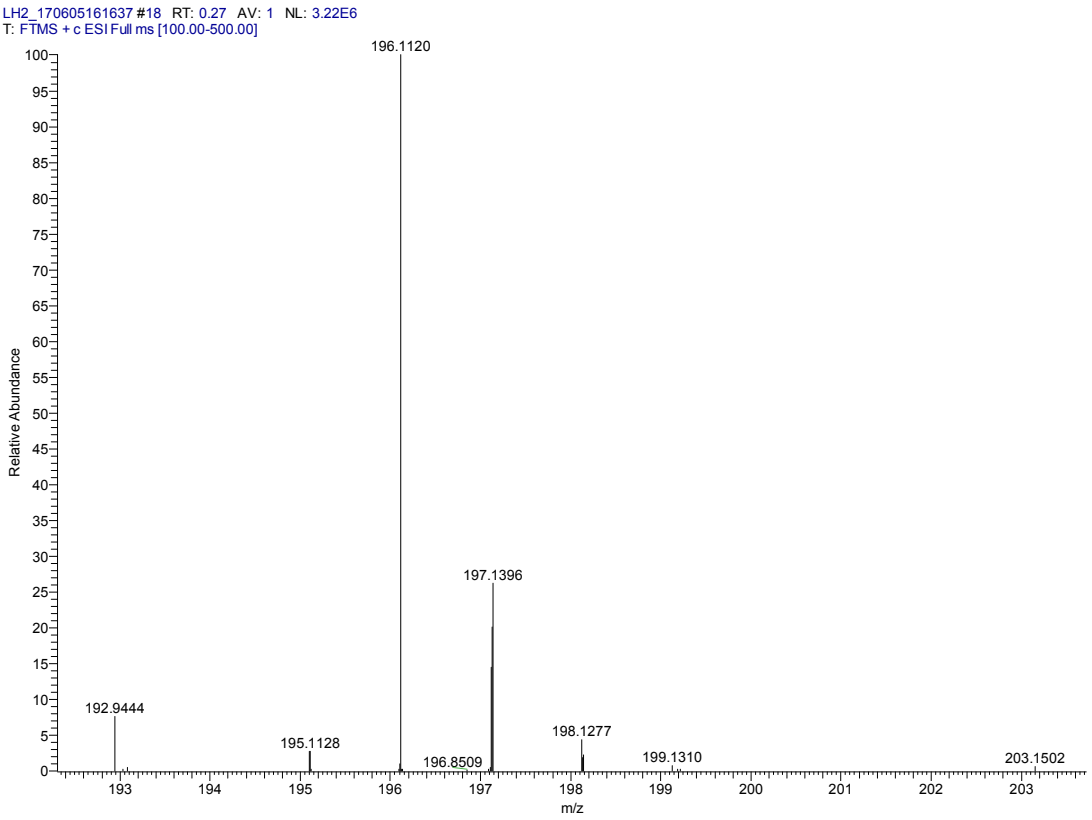

Fig. S25: ESI-Mass spectrum of L7

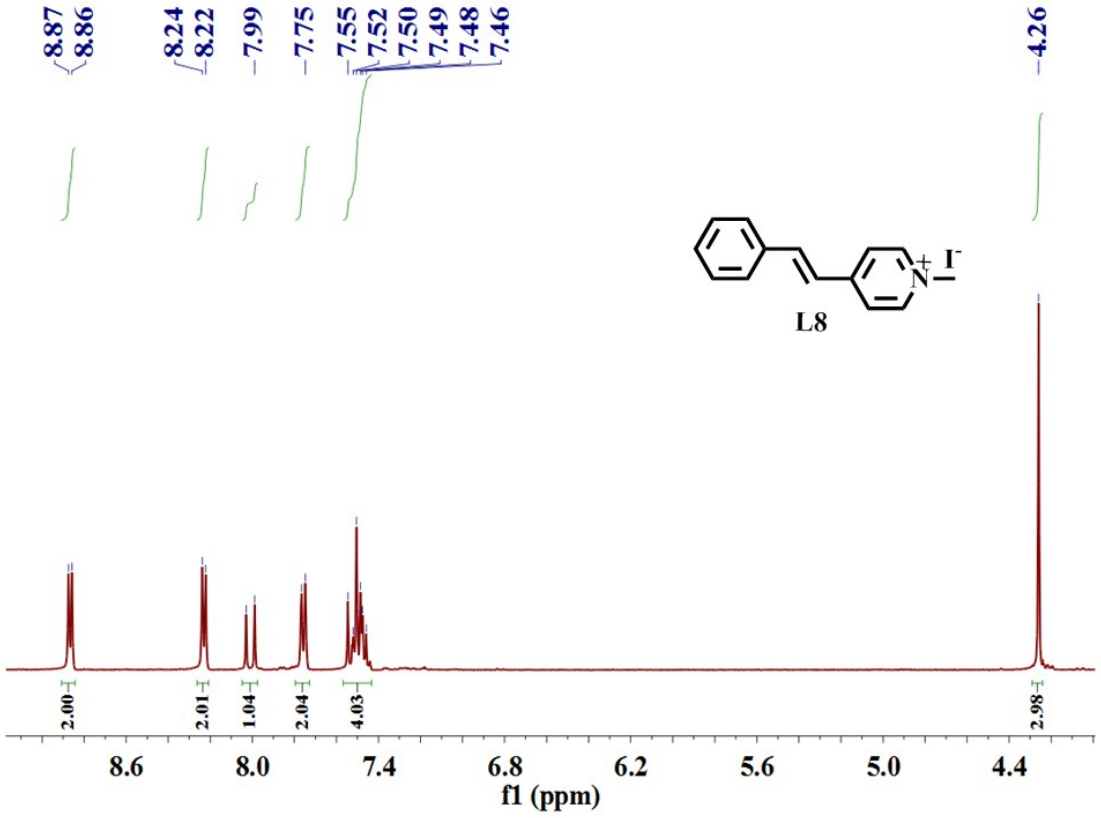

Fig. S26: ^{1}H NMR spectrum of L8 (DMSO-d_6)

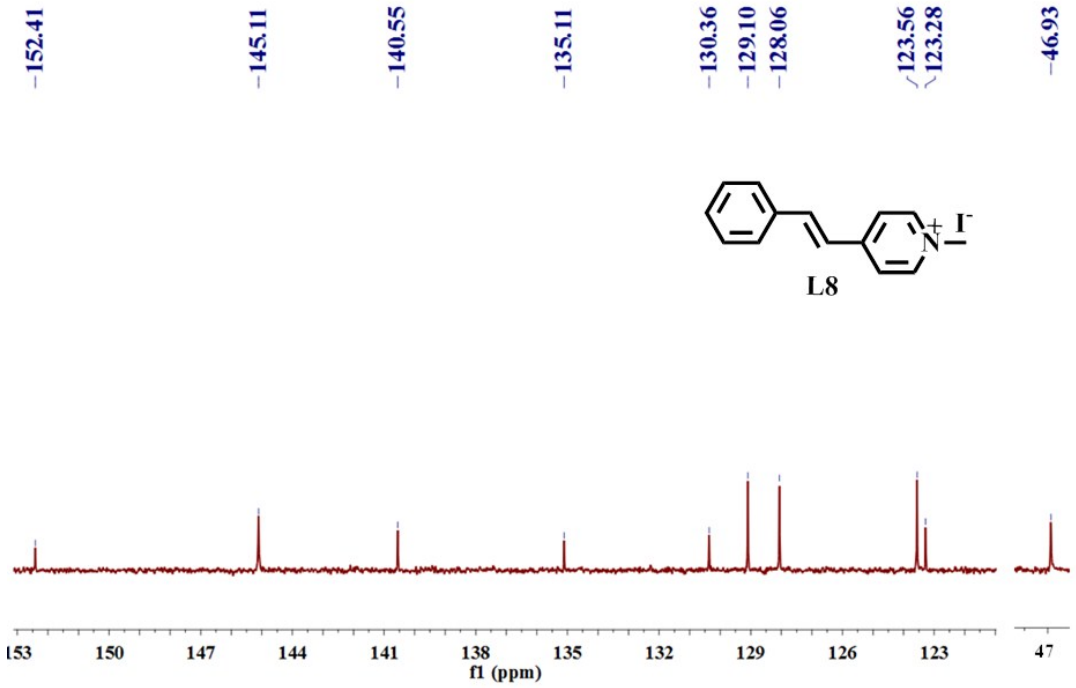

Fig. S27: ^{13}C NMR spectrum of L8 (DMSO-d_6)

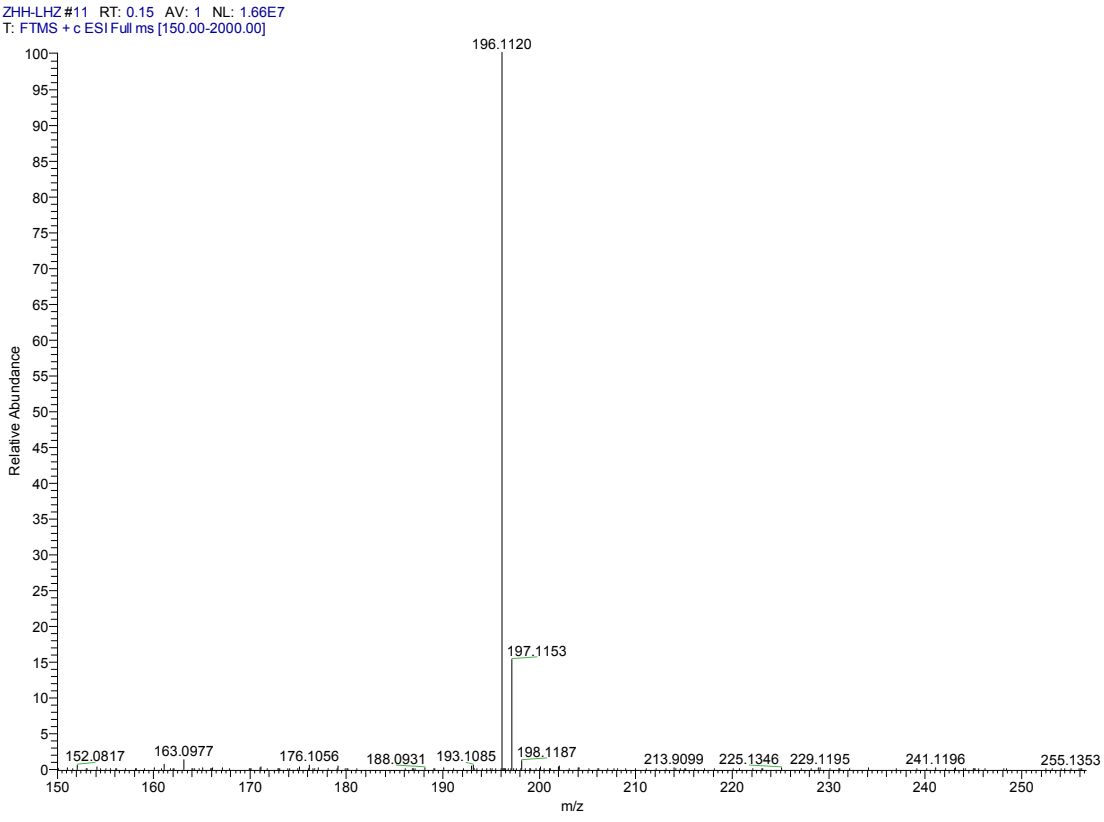

Fig. S28: ESI-Mass spectrum of L8

Photophysical Properties

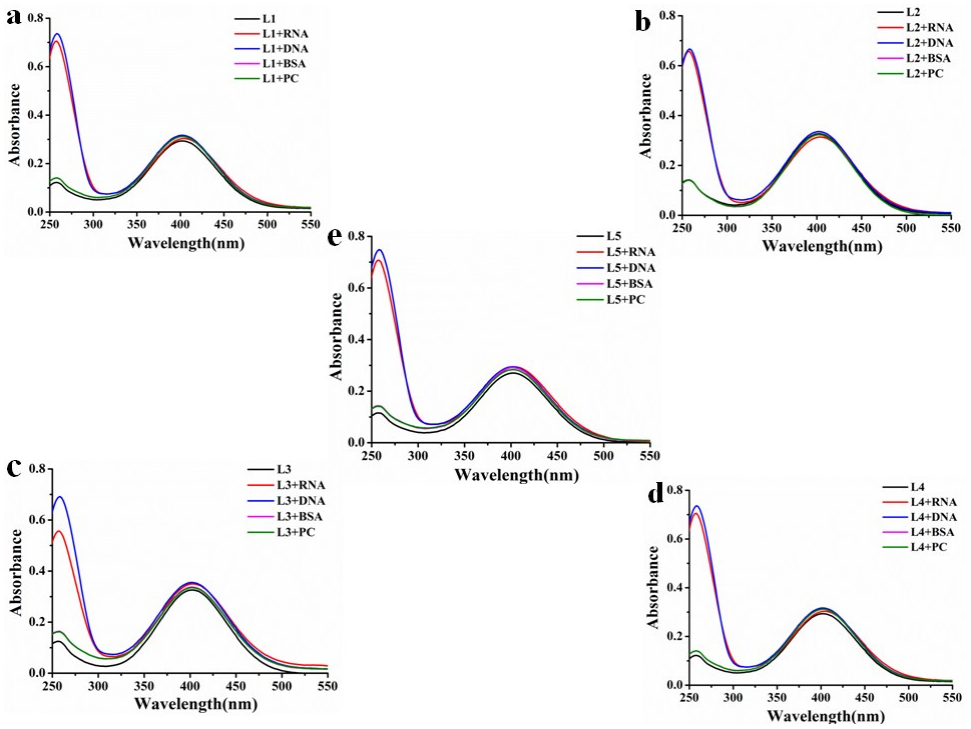

Fig. S29: UV-vis absorption spectra (a-e) of L1-5 (10 μM) and the mixture of L1-5 (10 μM) with10 eq. RNA, DNA, BSA and PC in Tris-HCl buffer (pH =7.4).

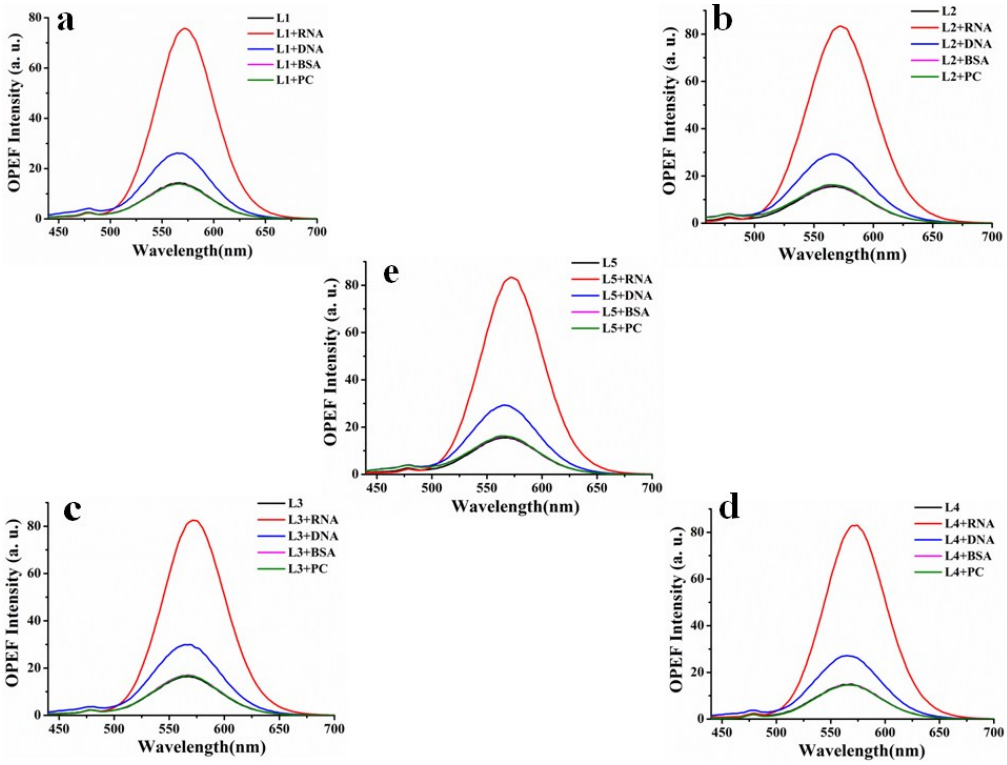

Fig. S30: One-photon excited fluorescence spectra (a-d) of L1-5 (10 μM) and the mixture of L1-5 (10 μM) with10 eq. RNA, DNA, BSA and PC in Tris-HCl buffer (pH =7.4).

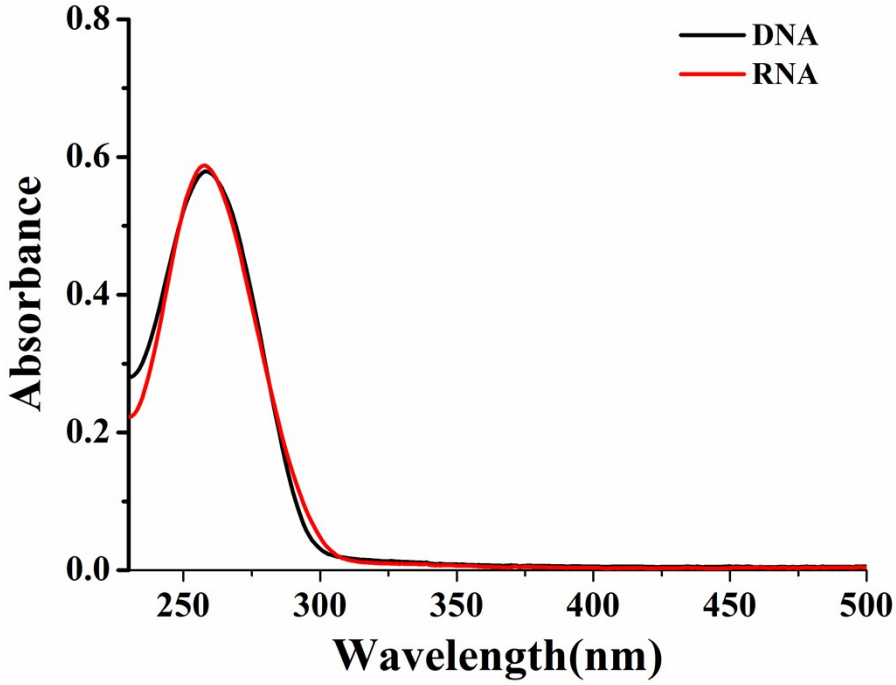

Fig. S31: UV-vis absorption spectra of RNA and DNA (1×10^{-4} M) in Tris-HCl buffer (pH =7.4)

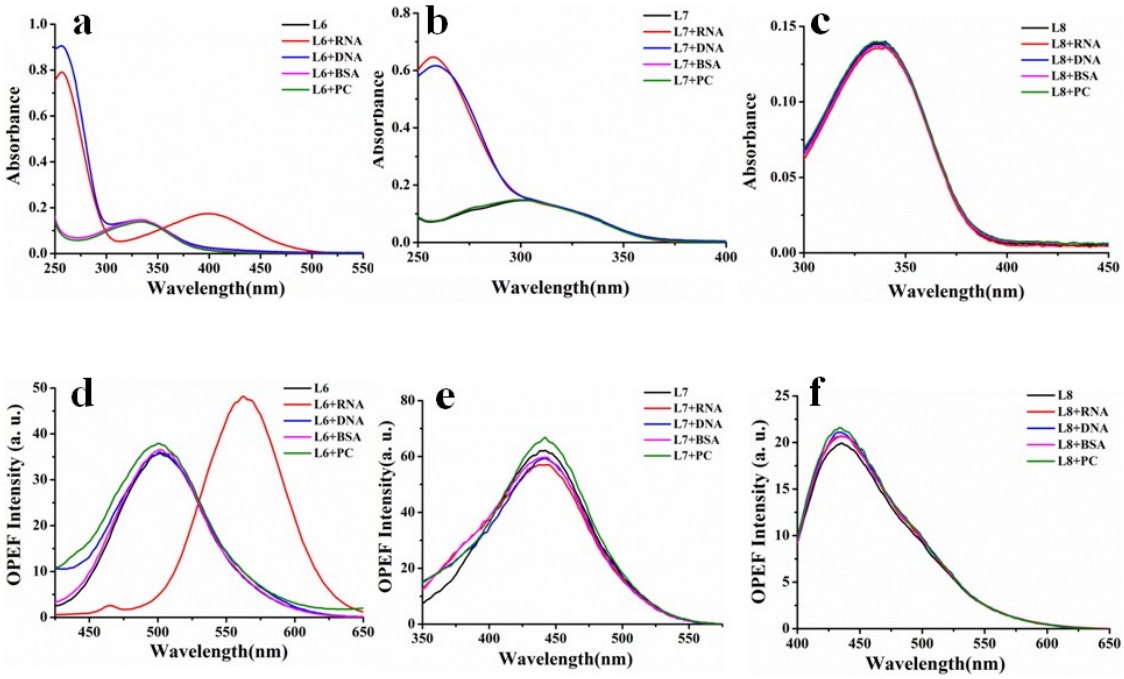

Fig. S32: UV-vis absorption spectra (a-c) and one-photon excited fluorescence spectra (d-f) of L6-8 (10 μM) and the mixture of L6-8 (10 μM) with 10 eq. RNA, DNA, BSA and PC in Tris-HCl buffer (pH =7.4).

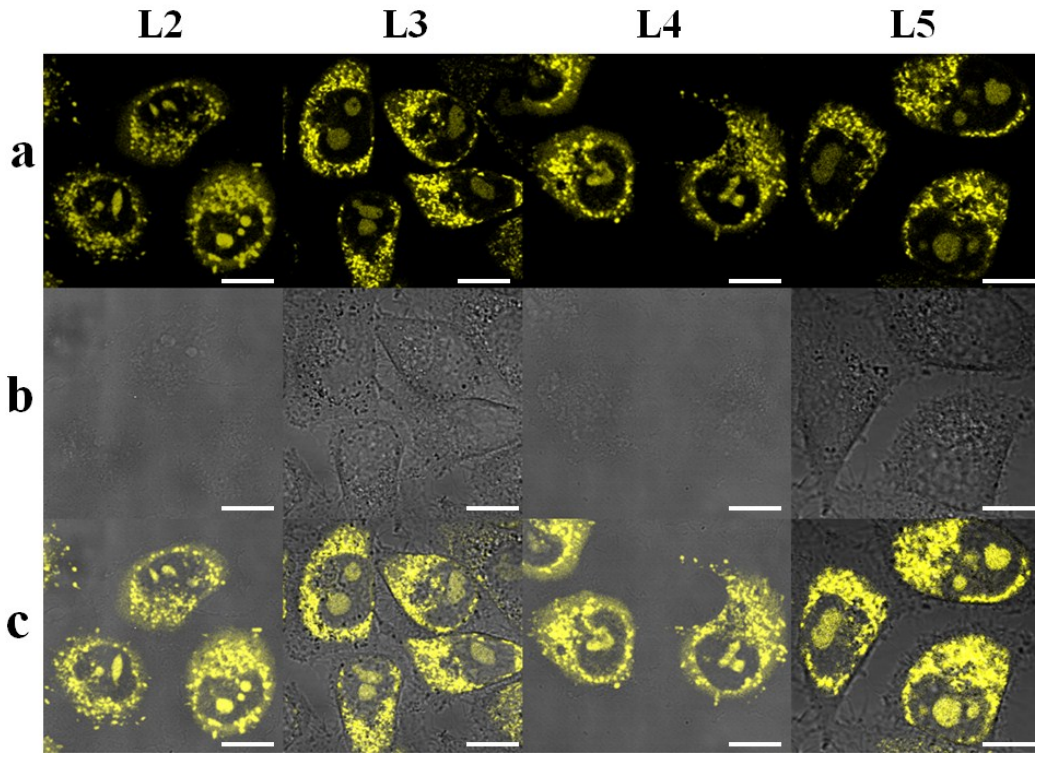

Fig. S33. The confocal fluorescence images of live HeLa cells stained with L2-5 (10 μM): (a) fluorescence images of L2-5 (λ_{ex} = 405 nm, λ_{em} = 550-600 nm); (b) bright- field images; (c) overlay of parts a and b. Scale bar: 20 μm.

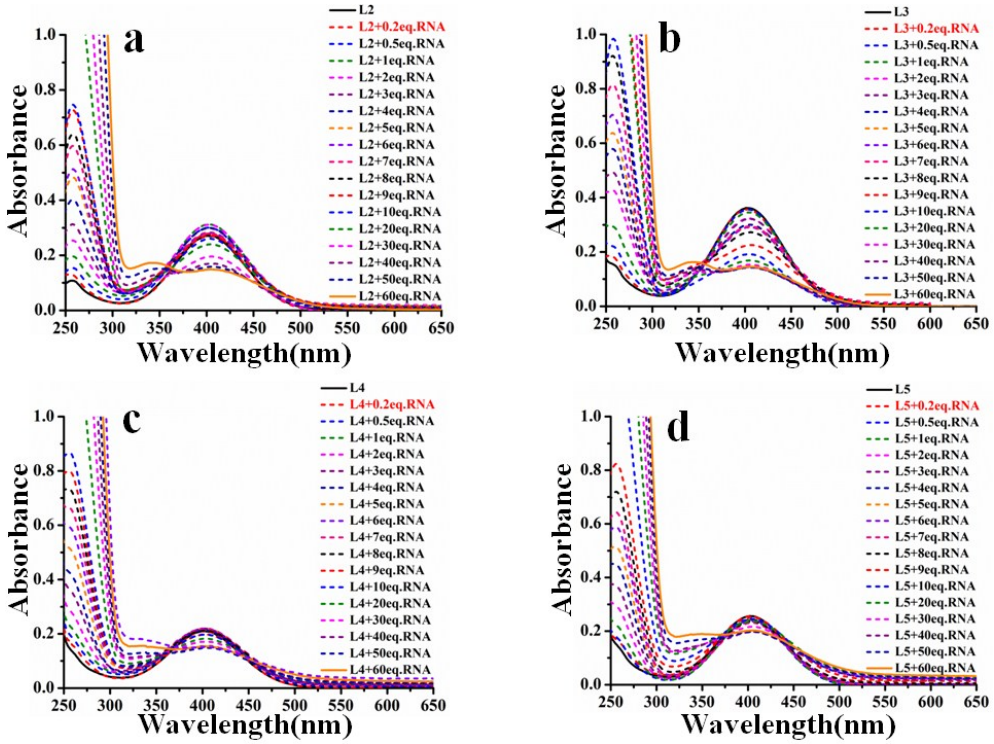

Fig. S34. UV-vis absorption spectra (a-d) of L2-5 under various amounts of RNA (0-60 equiv.) in Tris-HCl buffer (pH = 7.4).

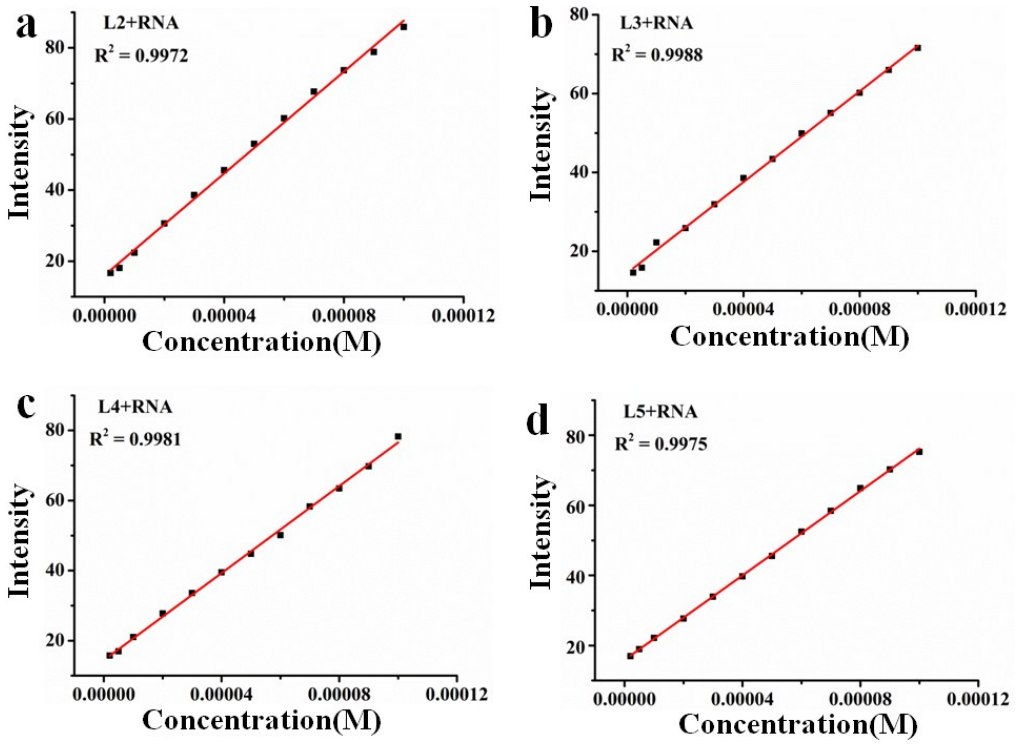

Fig. **S35**. One-photon excited fluorescence (OPEF) intensity (a-d) of L2-5 (10 μM) under various amounts of RNA (0-100 μM) in Tris-HCl buffer (pH = 7.4).

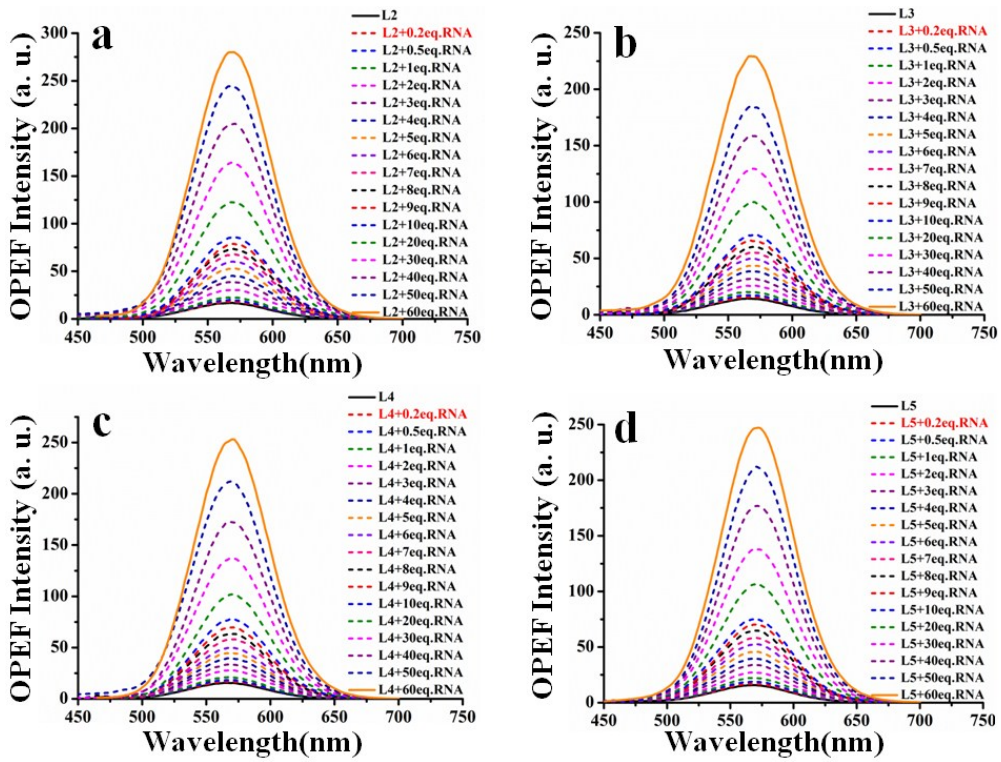

Fig. S36. One-photon excited fluorescence emission spectra (a-d) of L2-5 under various amounts of RNA (0-60 equiv.) in Tris-HCl buffer (pH = 7.4).

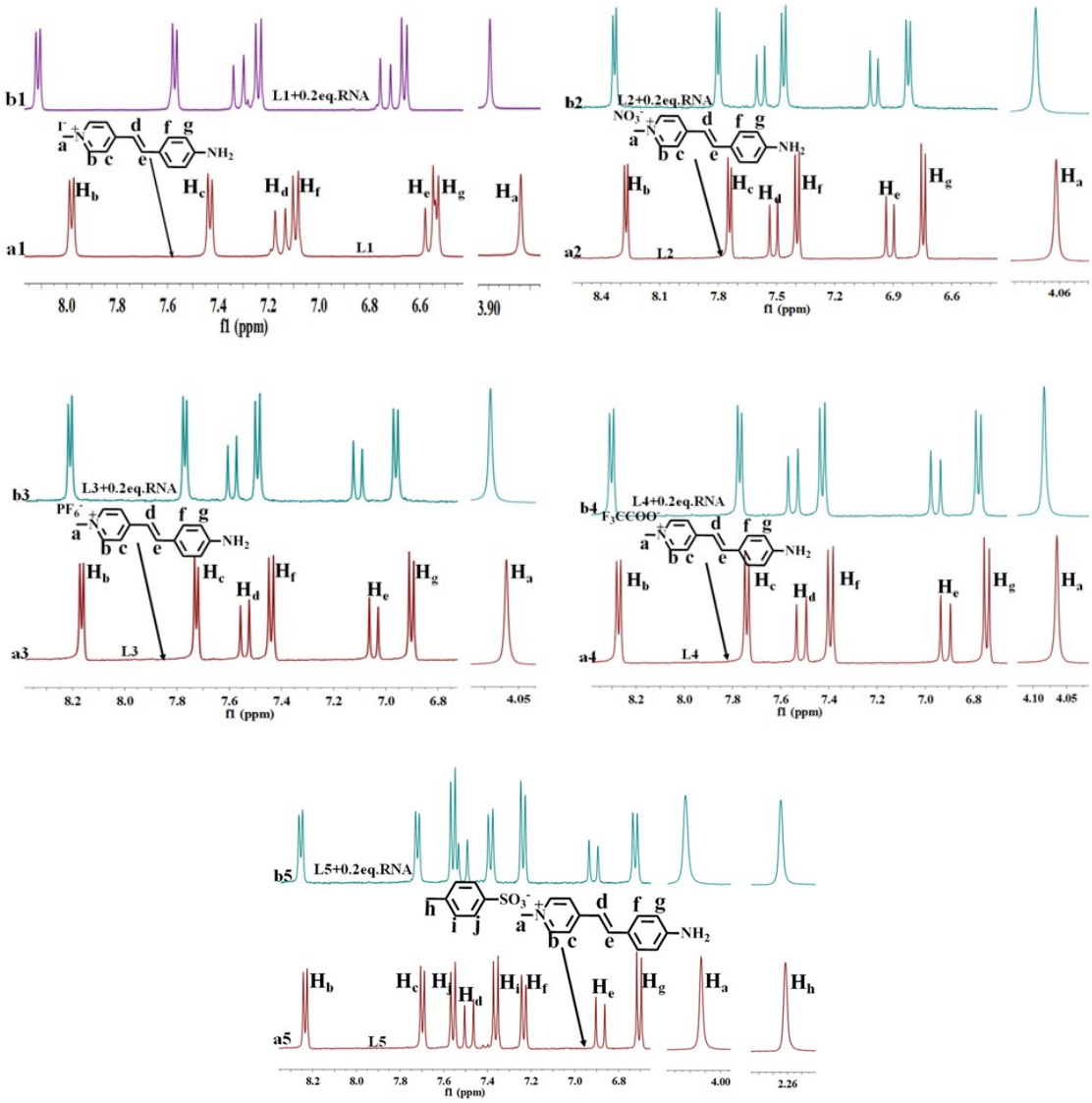

Fig. S37. ^{1}H NMR spectra of L1-5 upon titration with (a1-5) 0 equiv. (b1-5) 0.2equiv. of RNA in D_2O, respectively. RNA was dissolved in D_2O.

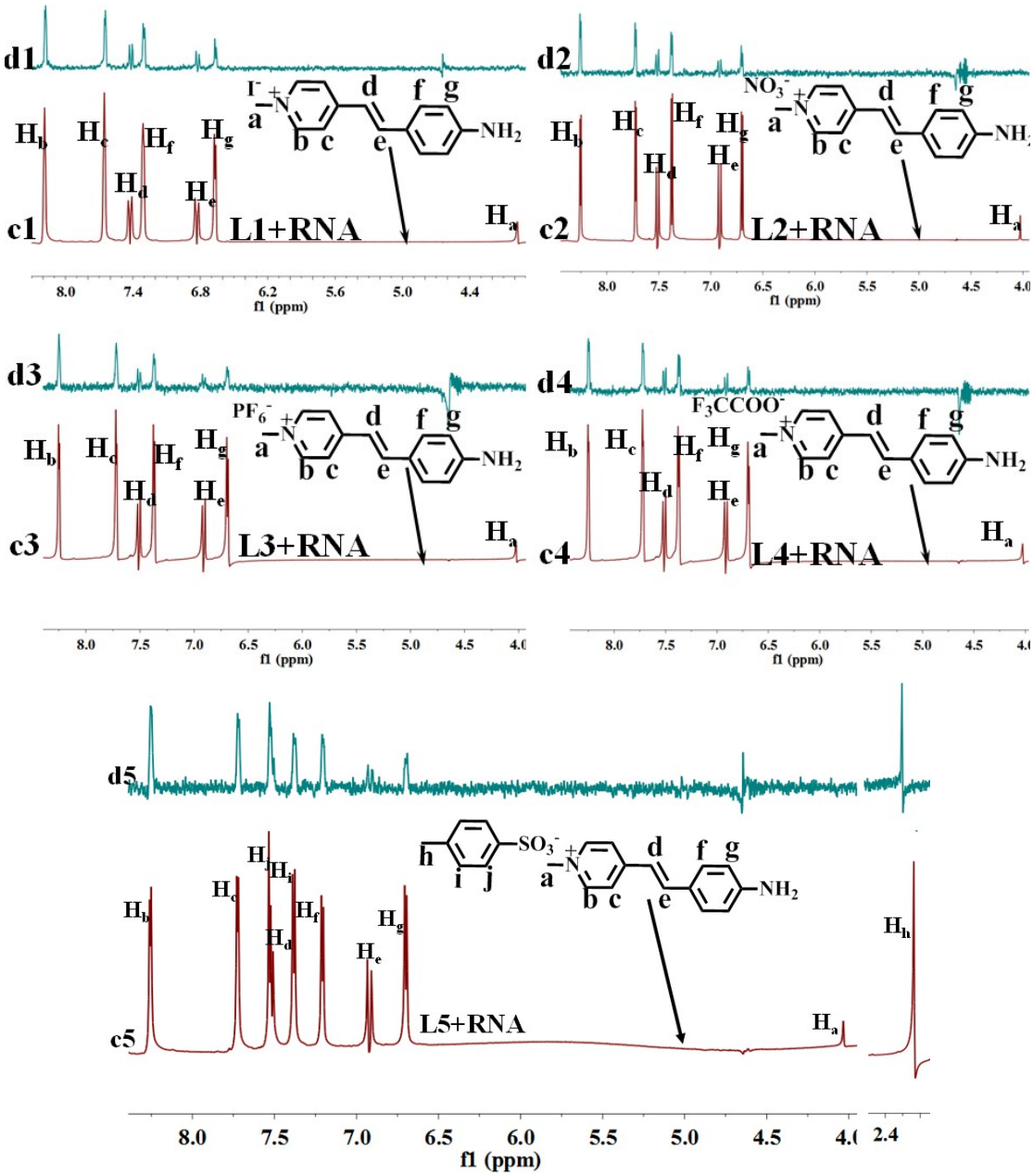

Fig. S38. (c1-5) Reference and (d1-5) STD NMR spectra of 50 μM RNA in the presence of 5 mM L1-5.

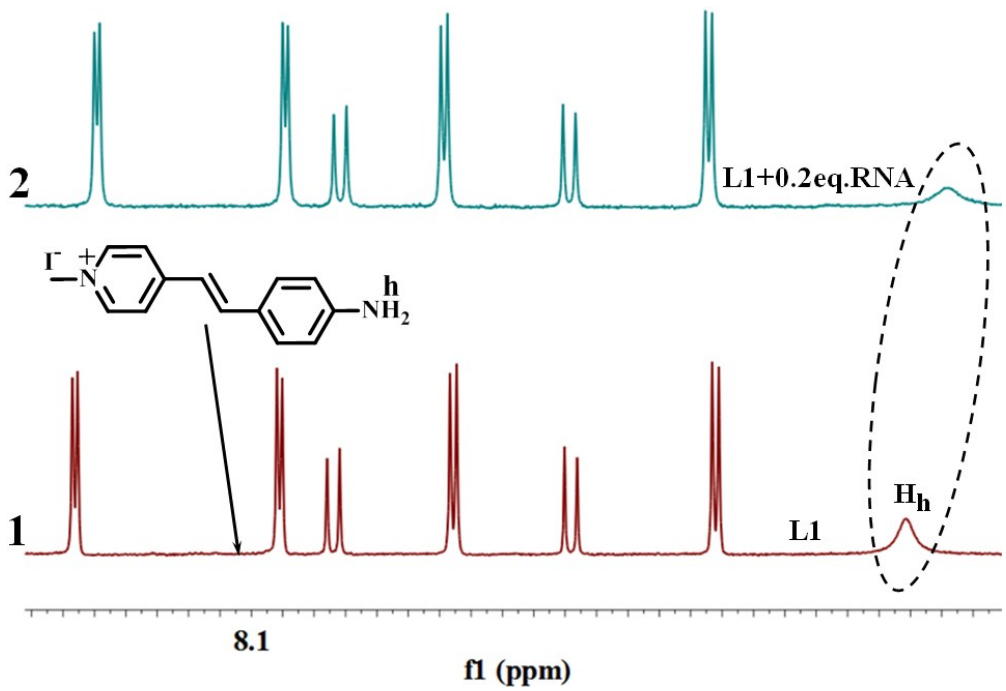

Fig. S39. ^{1}H NMR spectra of L1 upon titration with (1) 0 equiv. (2) 0.2 equiv. of RNA in DMSO-d_6; RNA was dissolved in D_2O.

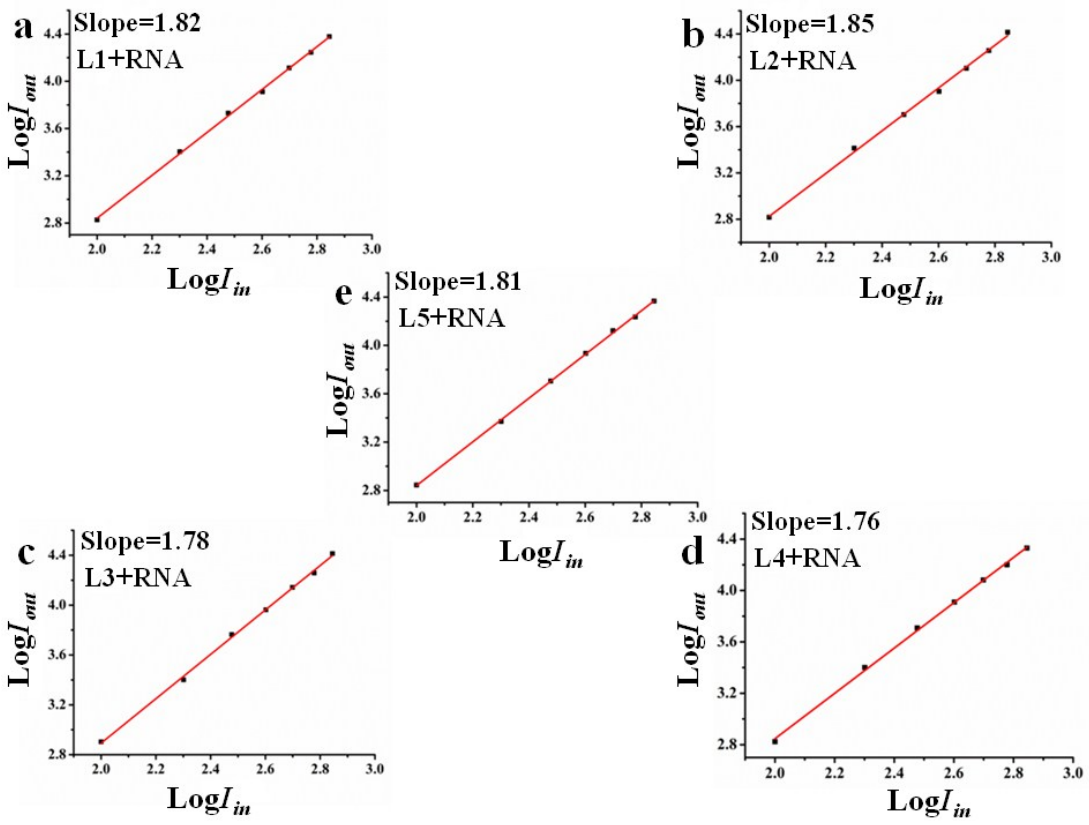

Fig. S40. The verification of two-photon excited fluorescence.

Table S1 The photophysical properties of L1-5

Comp.	solvent	λ_{abs}(nm)	λ_{em}(nm)	Stokes shift(nm)	ε	τ(ns)	Φ	$\sigma_{max/}$ GM	$\Phi\sigma_{max/}$ GM
L1	Buffer	403	567	164	2.67	0.01	0.007	0	0
L1+RNA	Buffer	418	570	152	1.83	1.78	0.107	154.09	16.49
L2	Buffer	402	567	165	2.72	0.03	0.006	0	0
L2+RNA	Buffer	415	570	155	1.88	1.84	0.108	149.70	16.17
L3	Buffer	403	567	164	2.63	0.01	0.005	0	0
L3+RNA	Buffer	414	569	155	1.82	1.83	0.105	147.77	15.52
L4	Buffer	402	568	166	2.65	0.01	0.008	0	0
L4+RNA	Buffer	416	570	154	1.89	1.73	0.107	147.20	15.75
L5	Buffer	403	567	164	2.69	0.01	0.007	0	0
L5+RNA	Buffer	415	572	153	1.85	1.75	0.106	153.95	16.32

Buffer is the Tris-HCl buffer (pH = 7.4), ε is the molar absorptivity (10^4 $M^{-1}cm^{-1}$), τ is fluorescence decay lifetime (ns), Φ is one-photon fluorescence quantum yield, σ_{max} is two-photon absorption cross-section determined using Rhodamine 6G as the standard at 820 nm. $\Phi\sigma_{max}$ is two-photon action cross-section determined using Rhodamine 6G as the standard at 820 nm. 1 GM = 10^{-50} $cm^4 \cdot s \cdot photon^{-1}$, RNA/L1-5 ratio: 60:1.

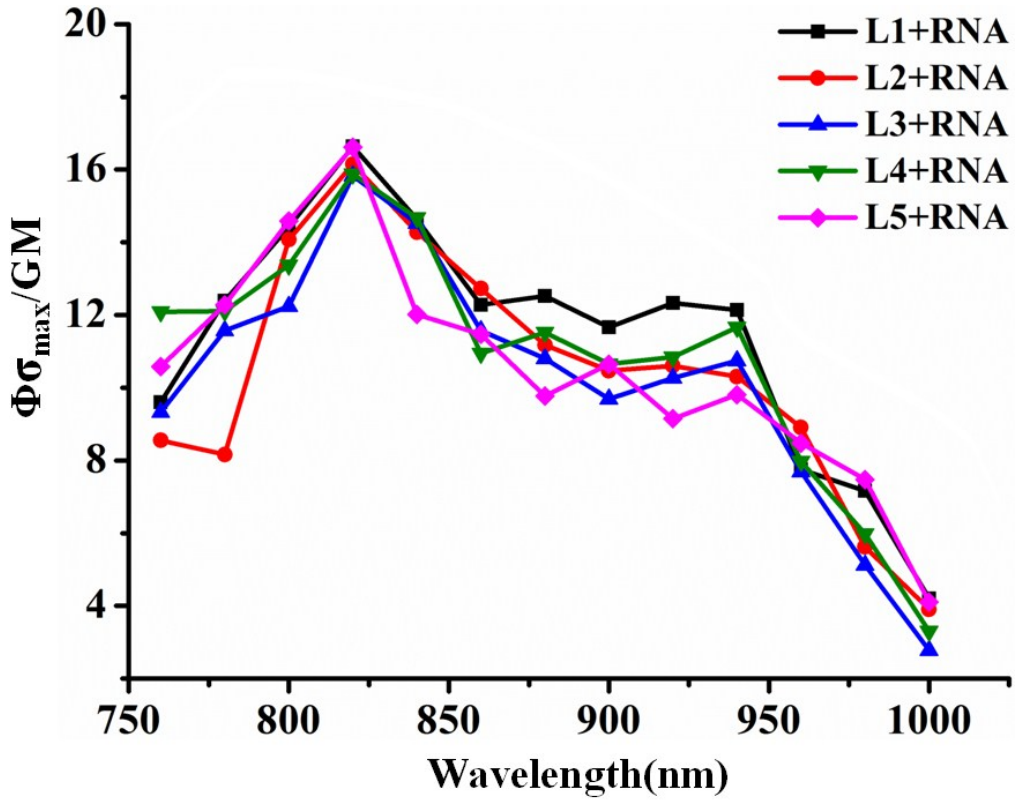

Fig.S41. Two-photon action cross-sections of L1-5 (0.1mM) in the presence of 60equiv. RNA.

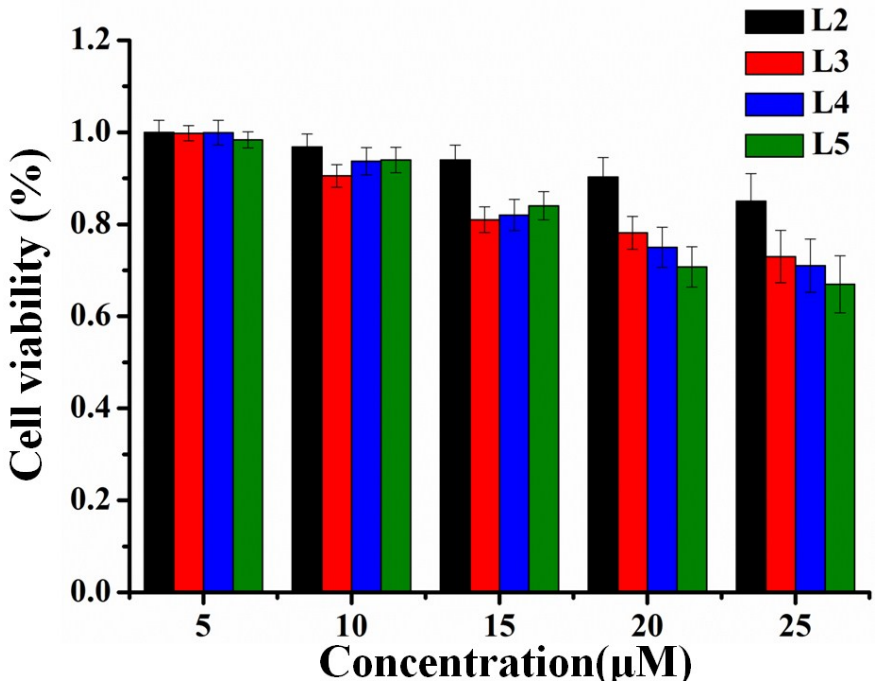

Fig. S42. MTT assay of HeLa cells treated with L2-5 at different concentrations for 24 h.

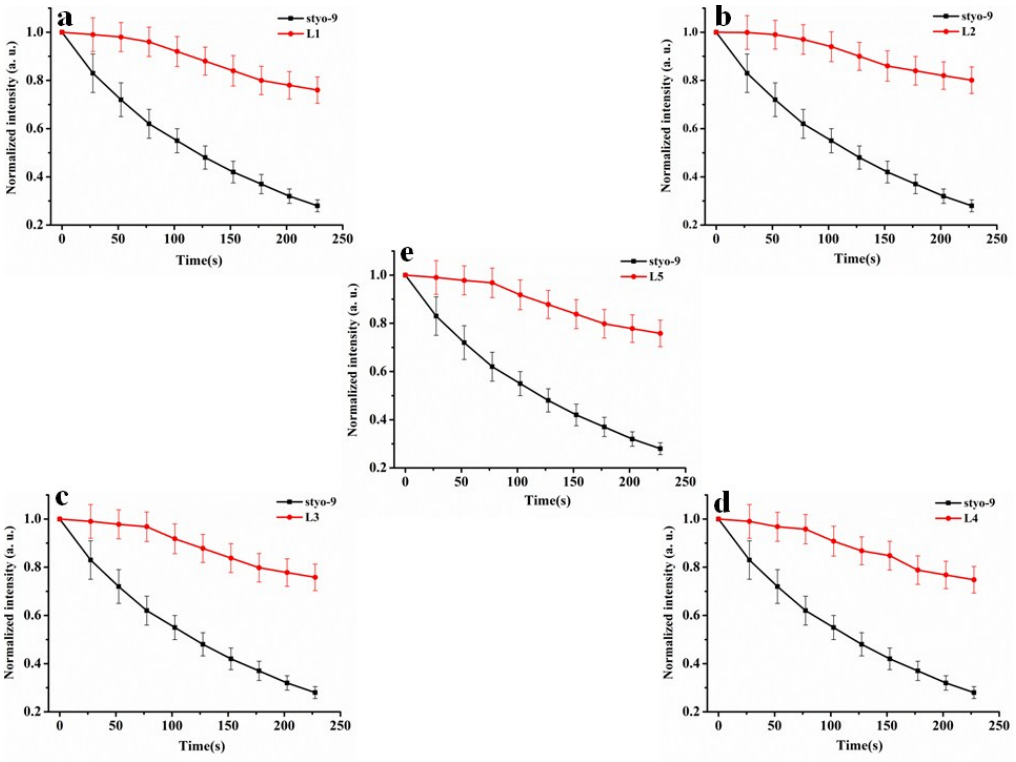

Fig. S43. Photostability of L1-5 and Syto-9 in cell imaging.

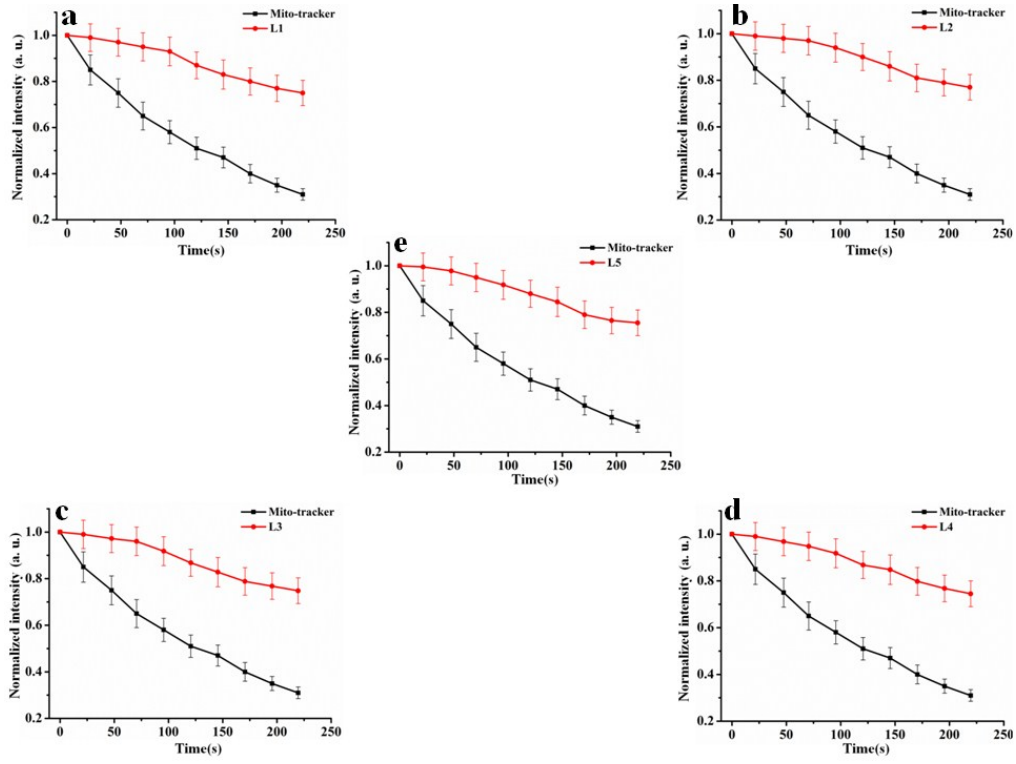

Fig. S44. Photostability of L1-5 and Mito-tracker deep red in cell imaging.

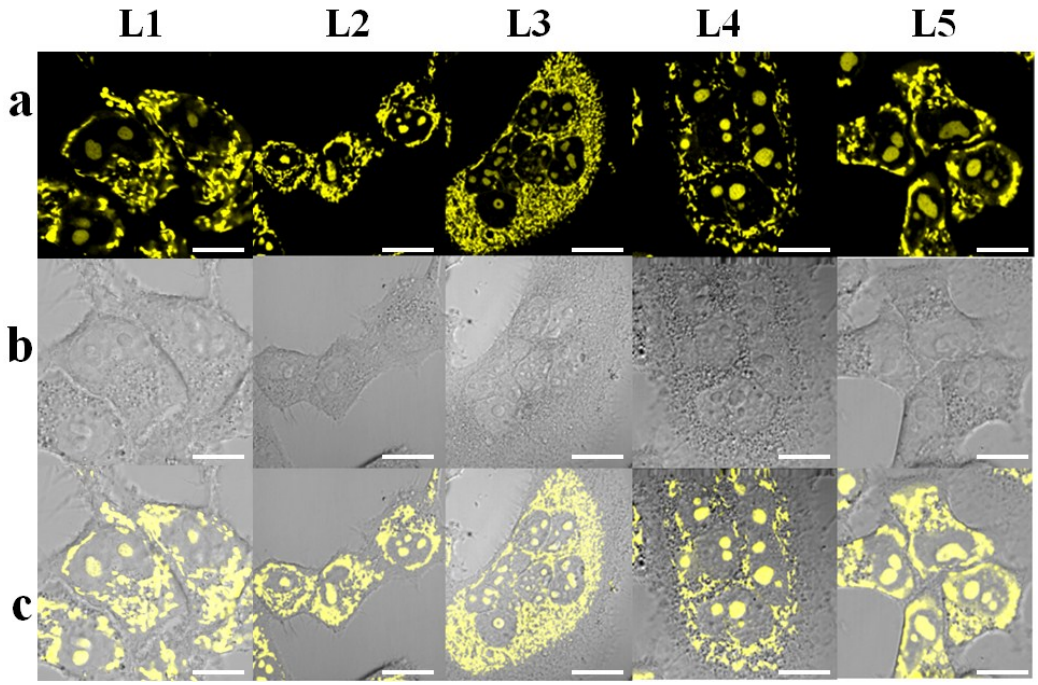

Fig. S45. Two-photon fluorescence images of live HeLa cells stained with L1-5 (10 μM): (a) fluorescence images of L1-5 (λ_{ex} = 820 nm, λ_{em} = 550-600 nm); (b) bright- field images; (c) overlay of parts a and b. Scale bar: 20 μm.

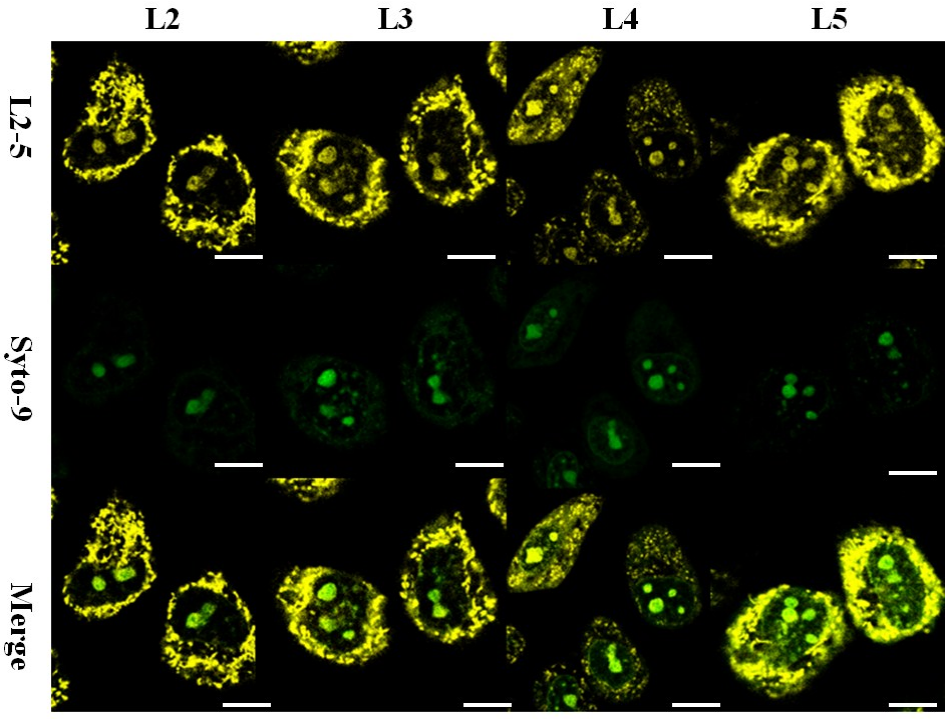

Fig. S46. Colocalization images of live HeLa cells with L2-5 (λ_{ex} = 820 nm, λ_{em} = 560-600 nm) and Syto-9 (λ_{ex} = 488 nm, λ_{em} = 500-540 nm), respectively. Scale bar: 20 μm.

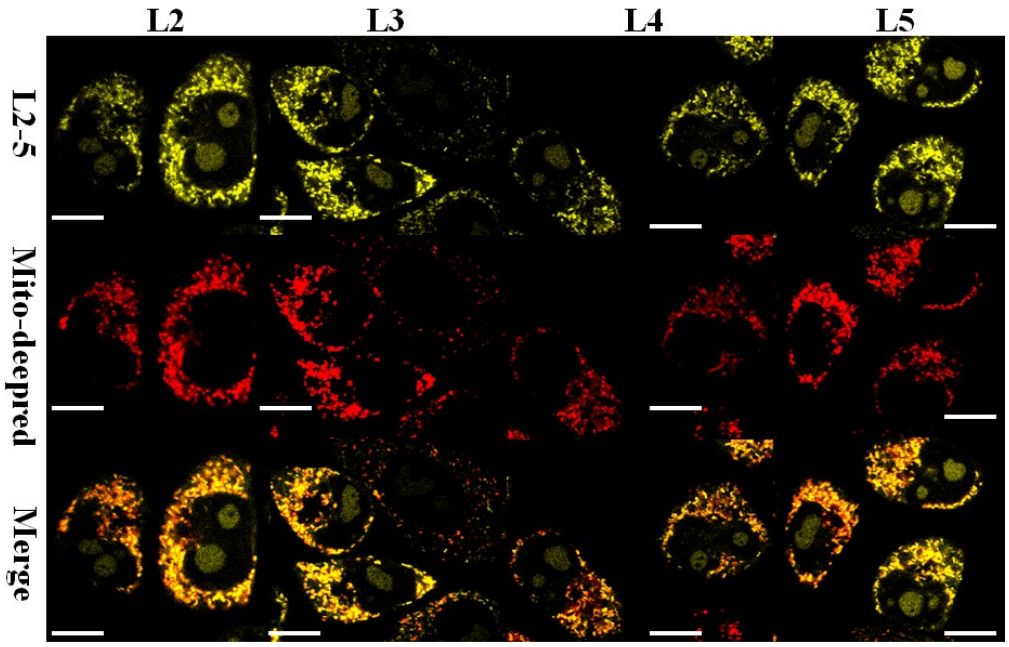

Fig. S47. Colocalization images of live HeLa cells with L2-5 (λ_{ex} = 820 nm, λ_{em} = 550-600 nm) and Mito-deep red (λ_{ex} = 633 nm, λ_{em} = 655-700 nm), respectively. Scale bar: 20 μm.

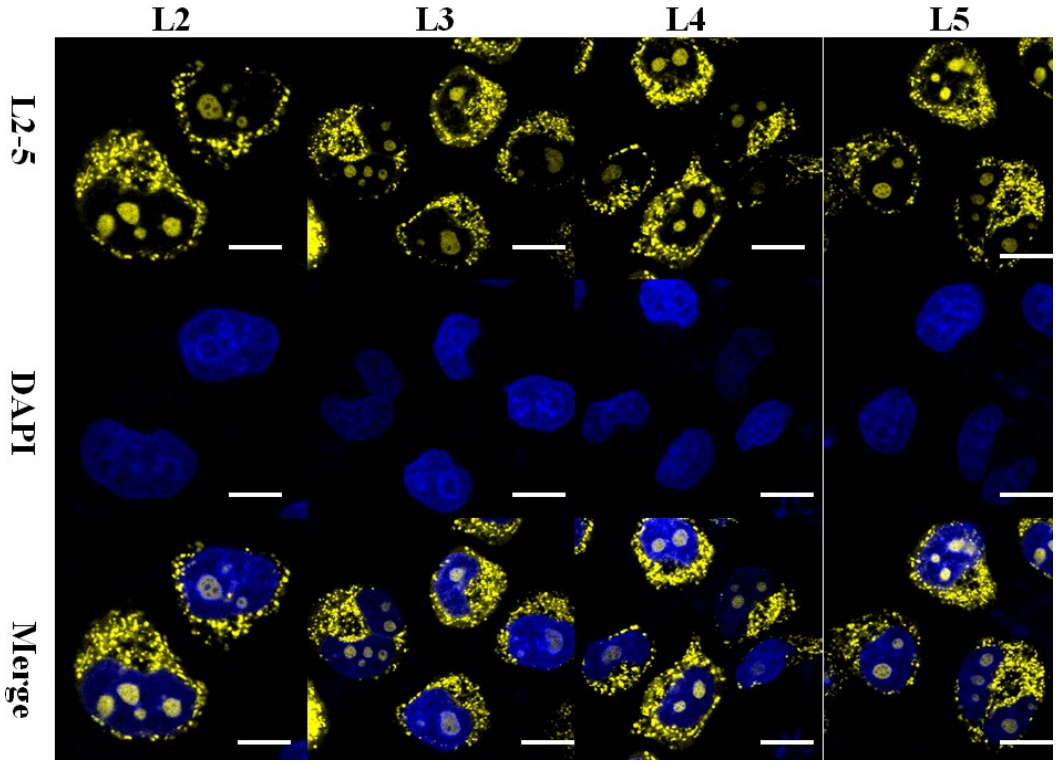

Fig. S48. Colocalization images of live HeLa cells with L2-5 (λ_{ex} = 820 nm, λ_{em} = 550-600 nm) and DAPI (λ_{ex} = 405 nm, λ_{em} = 425-490 nm), respectively. Scale bar: 20 μm.

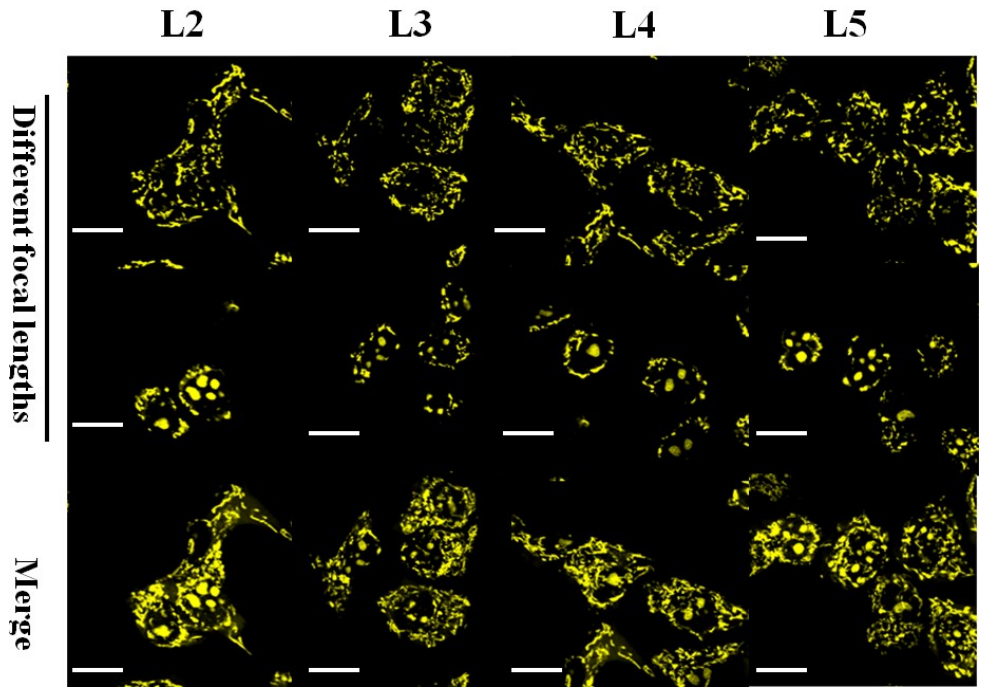

Fig. S49. Two-photon fluorescent images of live HeLa cells stained with L2-5 (10 μM) for 30 min under different focal lengths (λ_{ex} = 820 nm, λ_{em} = 550-600 nm). Scale bar is 20 μm.

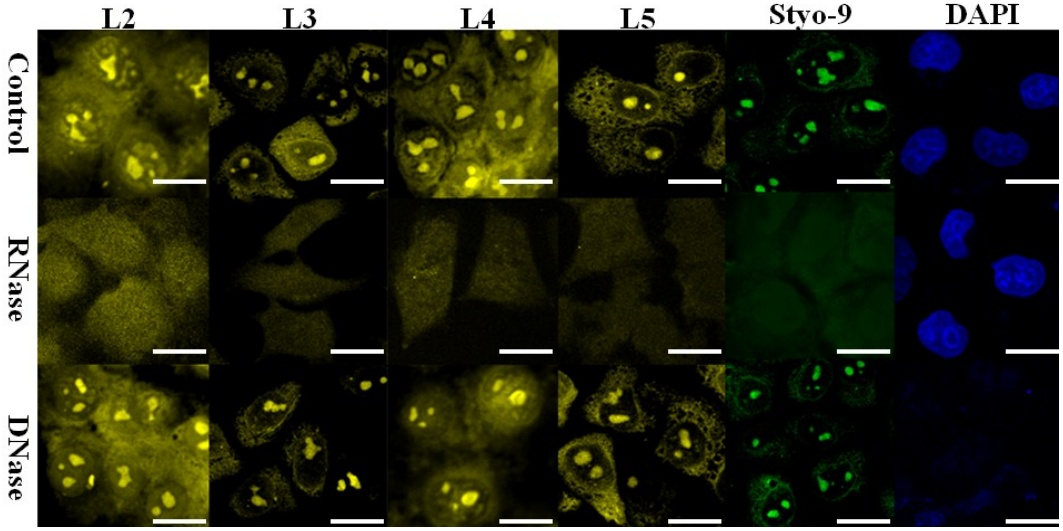

Fig. S50. DNase and RNase digest test images of fixed HeLa cells incubation with L2-5 (λ_{ex} = 820 nm, λ_{em} = 550-600 nm), Syto-9 (λ_{ex} = 488 nm, λ_{em} = 500-540 nm) and DAPI (λ_{ex} = 405 nm, λ_{em} = 425-490 nm). Scale bar: 20 μm.

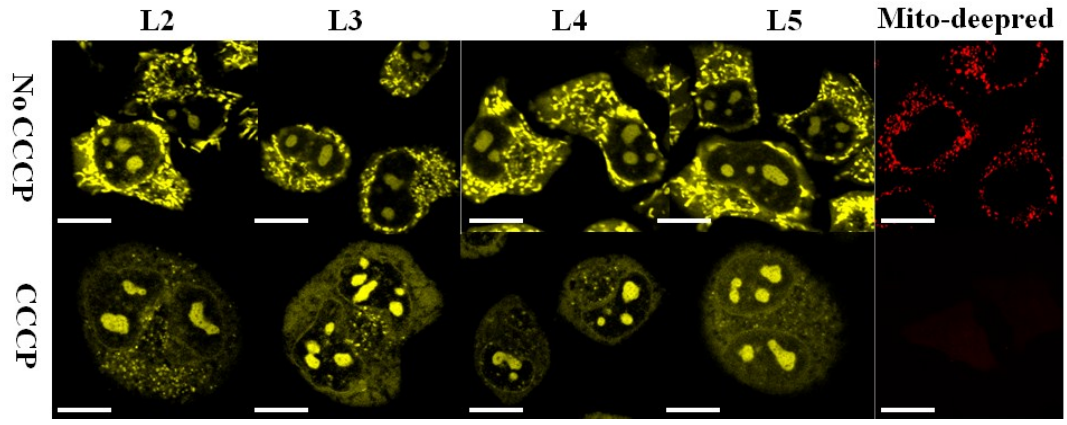

Fig. S51. Confocal laser fluorescence microscopy images of live HeLa cells treated with 10 μM L2-5 (λ_{ex} = 820 nm, λ_{em} = 550-600 nm) or 1.0 μM Mito-deep red (λ_{ex} = 633 nm, λ_{em} = 655-700 nm) and then incubated in the absence or presence of 10 μM CCCP for 10 min. Scale bar: 20 μm.

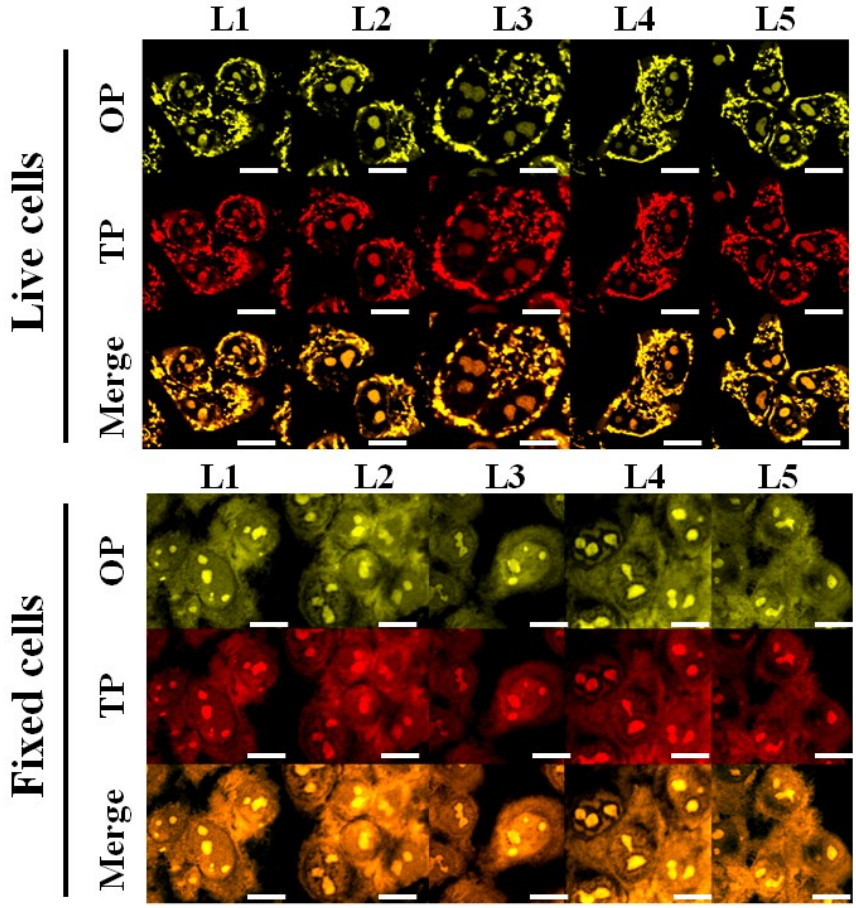

Fig. S52. One-photon (OP) and two-photon (TP) fluorescence microscopy images of L1-5 in live and fixed HeLa cells. One and two-photon excitation wavelength was at 405 and 800 nm, respectively. Scale bar: 20 μm.

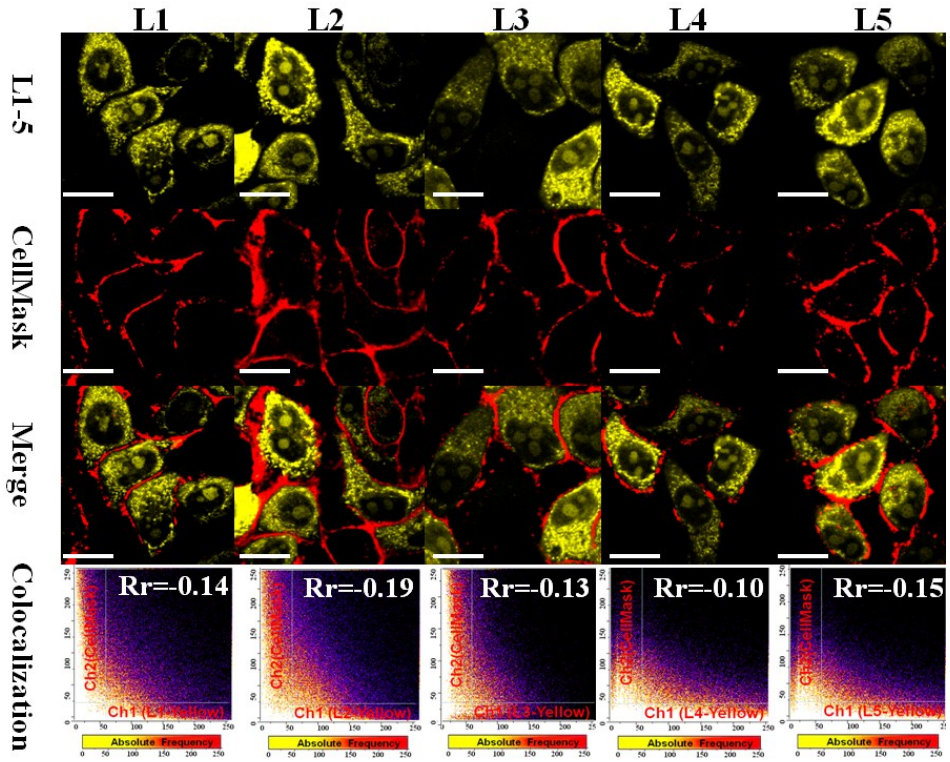

Fig. S53. Colocalization images of live HeLa cells with L1-5 and CellMask-Red (CellMask), respectively. Scale bar: 20 μm.

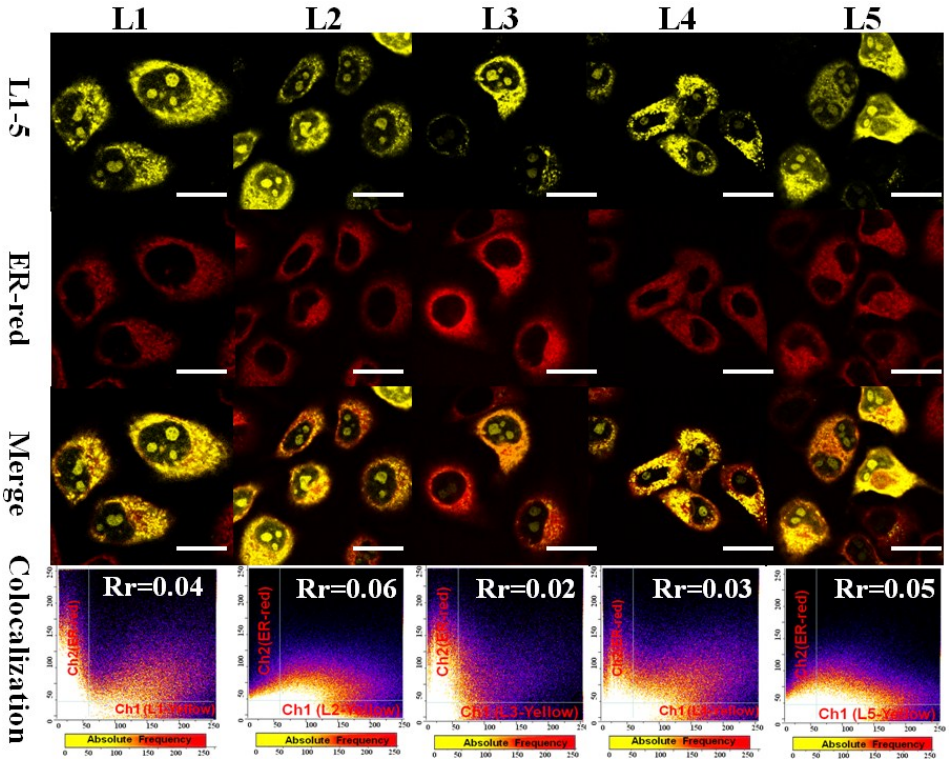

Fig. S54. Colocalization images of live HeLa cells with L1-5 and ER-Red, respectively. Scale bar: 20 μm.

Notes and references

1. Y. W. Tang, H. Liu, H. Zhang, D. D. Li, J. Su, S. Y. Zhang, H. P. Zhou, S. L. Li, J. Y. Wu, Y. P. Tian, *Spectrochimica Acta Part A: Molecular and Biomolecular Spectroscopy*, 2017, **175**, 92-99.
2. W. F. Niu, L. Guo, Y. H. Li, S. M. Shuang, C. Dong, M. S.Wong, *Anal. Chem.*, 2016, **88**, 1908-1914.
3. J. T. Pan, F. Tang, A. X. Ding, L. Kong, L. M. Yang, X. T. Tao, Y. P. Tian, J. X. Yang, *RSC Advances*, 2015, **5**, 191-195.
4. M. Jahan, Q. L. Bao, K. P. Loh, *J. Am. Chem. Soc.*, 2012, **134**, 6707-6713.
5. N. S. Makarov, M. Drobizhev and A. Rebane, *Optics Express*, 2008, **6**, 4029-4047